SCCWRP #1480

frontiers in Marine Science

TYPE Original Research
PUBLISHED 20 April 2026
DOI 10.3389/fmars.2026.1729816

OPEN ACCESS

EDITED BY
Raleigh Robert Hood,
University of Maryland, United States

REVIEWED BY
Vasco Manuel Nobre de Carvalho da Silva Vieira,
University of Lisbon, Portugal
Olaf Duteil,
Duteil Environmental Numerics, Germany

*CORRESPONDENCE
Fayçal Kessouri
faycalk@sccwrp.org

RECEIVED 21 October 2025
REVISED 25 February 2026
ACCEPTED 23 March 2026
PUBLISHED 20 April 2026

CITATION
Kessouri F, Sutula M, Smith J, McWilliams J, Sandoval-Belmar M, Bianchi D, Damien P, Ho M, Kudela R and Anderson C (2026) Anthropogenic, climate, and meso and submesoscale influences on diatom productivity in the Southern California Bight, with implications for domoic acid producing harmful algal blooms.
Front. Mar. Sci. 13:1729816.
doi: 10.3389/fmars.2026.1729816

Anthropogenic, climate, and meso and submesoscale influences on diatom productivity in the Southern California Bight, with implications for domoic acid producing harmful algal blooms

Fayçal Kessouri[1,2]*, Martha Sutula[1], Jayme Smith[1], James McWilliams[2], Marco Sandoval-Belmar[2], Daniele Bianchi[2], Pierre Damien[2], Minna Ho[1,2], Raphael Kudela[3] and Clarissa Anderson[4]

[1]Department of Biogeochemistry, Southern California Coastal Water Research Project, Costa Mesa, CA, United States, [2]Department of Atmospheric and Oceanic Sciences, University of California, Los Angeles, Los Angeles, CA, United States, [3]Biology and satellite oceanography, University of California, Santa Cruz, Santa Cruz, CA, United States, [4]Scripps Institution of Oceanography, University of California, San Diego, San Diego, CA, United States

Blooms of *Pseudo-nitzschia* (PN), a toxigenic marine diatom genus, produce the neurotoxin domoic acid (DA) that causes nearly annual shellfishery closures and wildlife illnesses and deaths within the Southern California Bight (SCB), an urbanized marine embayment supporting a coastal population of more than 23-million people. Understanding the mechanisms that control these DA-producing harmful algal bloom (HAB) events is essential for shifting from a reactive to an adaptive management approach, yet knowledge remains limited by gaps in observational data. Because DA-producing PN strains are part of the broader diatom community, this study used a validated coupled physical-biogeochemical model to disentangle the environmental drivers of diatom productivity and their influence on the risk of DA-producing HABs. Model simulations, with and without anthropogenically enhanced terrestrial nutrient sources, were used to (1) investigate spatial and temporal patterns governing diatom productivity, (2) evaluate how upwelling, cyclonic eddies, climate regimes, and local anthropogenic nutrients contribute to those patterns, and (3) quantify the relative contribution of natural versus anthropogenic forcing on the risk of DA-producing HABs and attribute effects to specific nutrient sources. Results show that diatom production is primarily controlled by upwelling and eddies that modulate the vertical delivery of dissolved inorganic nitrogen (DIN) to the surface; Climate regimes further modulate DIN fluxes by altering oceanic energy, upwelling strength, stratification, and nitracline depth. Vertically integrated DIN concentration, combined with a regional climate index, accounts for 85% of the interannual variability in annual maximum DA. Together, variability in these processes creates spatial and temporal gradients in diatom productivity that influence the likelihood of DA events. In the SCB nearshore, anthropogenic nutrient inputs are elevating diatom biomass by up to 45 percent over five years on average, and up to 67 percent in a single year. Applying a chlorophyll-a threshold associated with a 50 percent increased risk of DA detection, model results indicate that anthropogenic nutrient inputs have widened the natural ocean's window of opportunity for DA events by expanding their spatial footprint, seasonal duration, and intensity. This work highlights the coupled natural-human dynamics driving HAB risk and the value of numerical models for informing adaptive coastal management.

KEYWORDS

climate oscillations, diatoms, harmful algal blooms, human nutrients, submesoscale currents, upwelling

1 Introduction

Pseudo-nitzschia (PN), a genus of marine diatom, is one of the leading causes of toxic harmful algal blooms (HABs) that occur with nearly annual frequency in the California Current System (CCS; Figure 1), an upwelling-dominated eastern boundary current system (Lewitus et al., 2012; Smith et al., 2018). A majority of known PN species can produce domoic acid (DA), a potent neurotoxin that can cause wildlife illness and death and put humans at risk through consumption of shellfish via amnesic shellfish poisoning (Bates et al., 2018, 1989). DA accumulates via trophic transfer into pelagic and benthic food webs (Bates et al., 1989; Bejarano et al., 2008; Lefebvre et al., 2017), causing sickness and mass mortality events in a variety of marine animals including sea lions, sea otters, whales and seabirds (De La Riva et al., 2009; Gibble et al., 2021; Kvitek et al., 2008; K. A. Lefebvre et al., 2002; L. Lefebvre et al., 2002). PN blooms appear to be expanding in severity. In 2015, a PN bloom extending from Point Conception in Southern California to the Gulf of Alaska caused exceptionally high DA levels (McCabe et al., 2016). Annual DA events from 2022 through 2025 caused thousands of marine mammal strandings in the SCB (Beatriz and Eileen, 2023), which are among the most severe DA-related stranding events in the last 15 years (Smith et al., 2018).

Unraveling the mechanisms that control the frequency and intensity of diatom blooms dominated by DA-producing PN species is crucial for transitioning from a reactive to a proactive and adaptive management response to these HABs. These mechanisms can be categorized into three fundamental components: 1) environmental drivers that influence the productivity of diatoms, 2) factors that favor the development of PN blooms vis-à-vis its interactions with the larger plankton community, and 3) controls that regulate the magnitude of cellular toxin production during a PN bloom event. Many experimental and observational studies have focused on the latter two components (e.g., Lelong et al., 2012; Trainer et al., 2012; Bates et al., 2018; Smith et al., 2018; Sandoval-Belmar et al., 2023), the fundamental controls on diatom productivity and their connections to DA-producing HABs remain largely unexplored. In the southern CCS, where diatoms dominate primary productivity (Lassiter et al., 2006, Taylor and Landry, 2018), a synthesis of a decade of observational data suggested that drivers controlling diatom productivity also exert an important control on PN bloom dynamics Sandoval-Belmar et al., 2023, Figure 1). Chlorophyll-a (Chl-a), an indicator of total phytoplankton biomass, is consistently, positively correlated with DA events. The probability of detecting DA rises above 50% at chlorophyll-a thresholds ranging from 1.8 mg m^{-3} in the Santa Barbara Channel in the SCB to 5.5 mg m^{-3} in Monterey Bay, California.

Factors that have linked to DA events in observational studies are also known to modulate diatom productivity. Observed DA has been strongly correlated with upwelling, climate regime, temperature, macronutrient ratios, wastewater, and riverine inputs, among other drivers in explaining the variance in observed DA concentrations in the southern CCS (Sandoval-Belmar et al., 2023). Oceanographic conditions in this region are highly dynamic due to the confluence of large-scale climate variability (e.g., El-Niño–Southern Oscillation [ENSO], Pacific Decadal Oscillation [PDO], North Pacific Gyre Oscillation [NPGO]), mesoscale eddies, and submesoscale turbulence, all of which have been observed to modulate nutrient fluxes and phytoplankton growth (McClatchie et al., 2008). Climate-driven changes in stratification, mixed-layer depth, and upwelling intensity directly impact the vertical flux of nutrients, altering primary production patterns (García-Reyes and Largier, 2012; Kahru et al., 2018). Additionally, wind stress curl plays a significant role in modulating nutrient upwelling and diatom blooms by generating Ekman pumping, which enhances subsurface nutrient entrainment and fosters localized productivity hotspots (Capet et al., 2008; Chelton et al., 2004; Kessouri et al., 2022). Terrestrial anthropogenic nutrient inputs, such as wastewater effluent and non-point source runoff from urban and agricultural landscapes, can enhance productivity (Kessouri et al., 2021a) and shift community composition (Heisler et al., 2008; Glibert et al, 2017). Their footprint is highly variable along the coast, further complicating driver attribution (Howard et al., 2017). However, these relationships are correlative, and observations alone cannot be used to quantify the relative importance of natural oceanic versus anthropogenic nutrients. Moreover, substantial gaps in observational records make their use in understanding drivers limited.

Mechanistic numerical models are the appropriate tool to disentangle the relative importance of natural oceanic versus anthropogenic forcing on diatom productivity and investigate the mechanisms for specific environmental drivers. Ocean biogeochemical models have advanced in the CCS to adequately represent the dynamic effects of biogeochemistry on lower trophic levels in coastal ecosystems, including controls on diatom

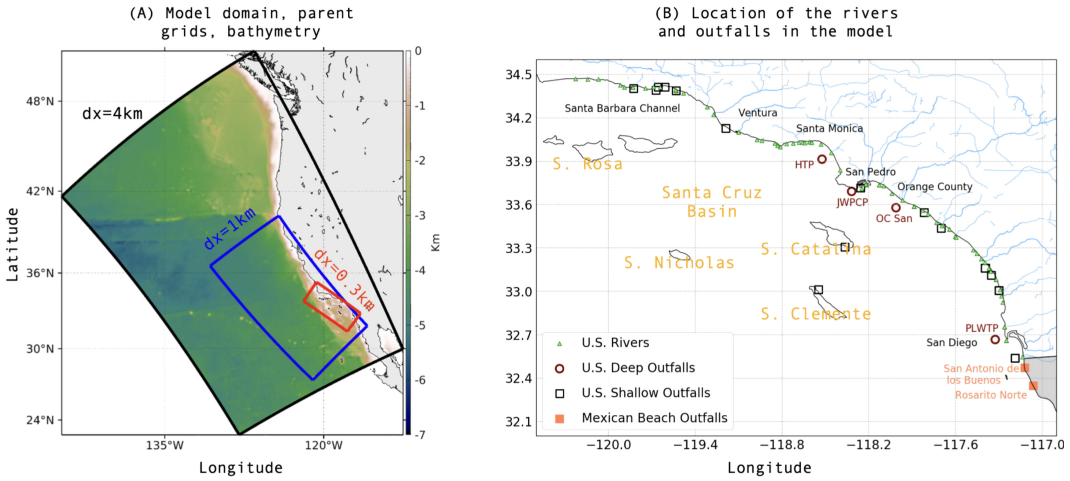

FIGURE 1
(A) Map of the location and downscaling steps from a 4 km resolution US West coast ROMS-BEC configuration, down to a 0.3 km configuration in the SCB. **(B)** Locations of the simulated U.S. rivers, publicly owned treatment works outfalls, and two beach outfalls from the Mexican coast.

production (Moore et al., 2004; Deutsch et al., 2021). In addition, recent advances in high-resolution coupled physical-biogeochemical models allow for unprecedented insights into the major processes. For example, numerical modeling studies have revealed that submesoscale fronts and filaments significantly contribute to nutrient redistribution and bloom formation (Lévy et al., 2024, 2018). More recently, models have been used to explicitly quantify the role of anthropogenic nutrient inputs in enhancing coastal primary productivity and its effect on increased respiration, acidification and hypoxia (Kessouri et al., 2021a, 2024, Frieder et al., 2024). An opportunity now exists to use numerical models to investigate how anthropogenic versus natural processes control diatom productivity and how this might also modulate the window of opportunity for DA-producing HABs.

In this study, we used a submesoscale resolving oceanic model to elucidate the relative role of natural oceanic and anthropogenic drivers in controlling diatom production and how this modifies the risks for toxic PN blooms. We focus this assessment on the Southern California Bight (SCB), an open coastal system located between the Baja California Peninsula and Point Conception in the Southern CCS. This region hosts a variety of marine communities and hotspots of biodiversity and Marine Protected Areas (Rassweiler et al., 2012). It is also home to a population of more than 23 million people, distributed along the coastline from Tijuana to Santa Barbara. Point and nonpoint source discharges to the ocean from this population are partitioned across 75 U.S. rivers, 19 ocean outfalls that discharge primary- and secondary-treated effluent from 23 wastewater treatment plants, which release, on average, 8 million m^3 d^{-1} of nutrient-enriched water to the ocean (Sutula et al., 2021; Figure 1). Discharges from growing coastal population in Tijuana and Baja California Mexico further increase nutrient pollution in the SCB. This study can provide a complementary line of evidence to ongoing observations and PN modeling studies that are investigating drivers of DA events (Sandoval-Belmar et al., 2026). We sought to: (1) document the temporal and spatial variability of diatom productivity in the SCB over a 20-year period (1997-2017), (2) investigate the relative influence of natural (upwelling and cyclonic eddies) versus anthropogenically enhanced terrestrial nutrient inputs on diatom productivity, and how these influences are modulated by climate regime, and (3) quantify how U.S. and Mexican pathways of anthropogenic nutrient inputs modulate the window of opportunity for DA-producing HABs, both in terms of spatial footprint as well as duration and intensity of potential bloom events, over a baseline of natural occurrence.

2 Materials and methods

2.1 ROMS-BEC model and configuration

We employed the Regional Oceanic Modeling System (Shchepetkin and McWilliams, 2005) coupled with the Biogeochemical Elemental Cycling model (Moore et al., 2004) (ROMS-BEC) to simulate physical and biogeochemical processes in the SCB. BEC resolves multiple elemental cycles (C, N, P, O, Fe, Si), three phytoplankton groups (diatoms, small phytoplankton, and diazotrophs), one zooplankton group, and detritus. The model represents sediment remineralization, mineral ballast sinking, carbonate chemistry, and air–sea gas exchange (Wanninkhof, 1992). The model tracks separate state variables for phytoplankton carbon (C) and chlorophyll for each functional group (and silica for diatoms), so C:Chl emerges from environmental conditions rather than being fixed. Growth follows balanced stoichiometry (C:N:P = 117:16:1), while photoacclimation adjusts chlorophyll per unit carbon in response to light and nutrient limitation, producing spatial and temporal variability in C:Chl. The C:Chl ratio is dynamically diagnosed using a Geider-type photoacclimation and balanced-growth framework. Although C, N, P, Si, Fe, and O cycles are explicitly represented, their uptake within each group is mechanistically coupled. Growth is carbon-based and regulated by nutrient limitation (N, P, Fe, and Si for diatoms), so elemental assimilation occurs in a coordinated manner governed by shared stoichiometric and physiological constraints. Detailed description and equations can be found in the supplemental documentation of Deutsch et al. (2021).

The SCB model domain spans from Tijuana to Pismo Beach and extends 200 km offshore, using one-way downscaling from 4 km (Deutsch et al., 2021) to 1 km (Kessouri et al., 2020) to 0.3 km (Kessouri et al., 2021b)horizontal resolution. One-way offline nesting is implemented following the procedures described by Mason et al. (2010), in which the parent grid is integrated independently and provides time-varying lateral boundary conditions to the child grid without feedback. Boundary conditions for free surface height, three-dimensional velocity, temperature, salinity, and biogeochemical tracers are extracted from the parent simulation, spatially and temporally interpolated onto the child grid, and applied using ROMS radiation–nudging open boundary conditions to ensure numerical stability and dynamical consistency across grid interfaces. This approach preserves large-scale circulation and tracer gradients imposed by the parent solution while allowing the nested grids to internally generate higher-resolution dynamics, enabling explicit representation of mesoscale and submesoscale processes in the innermost domain.

The high-resolution 0.3 km grid captures fine-scale dynamics, including eddies and coastal fronts, with 60 sigma vertical levels that encompass the entire water column of the domain, extending to a depth of 3875 meters. The bottom topography of the domain was generated using a 30-meter (1-arc) gridded bathymetric resolution product from the (NOAA National Geophysical Data Center, 2003). The model was run after a four-year spin-up, with 30-second time steps and the Weather Research Forecast (WRF)-derived (Skamarock et al., 2008) hourly forcing at 6 km resolution, including wind–current coupling parametrization (Renault et al., 2016, 2021). ROMS and the embedded BEC module were coupled online and advanced on the same 3-D (baroclinic) time step; physical transport (advection/mixing) and biogeochemical source-sink tendencies were updated each baroclinic step without offline coupling or independent biogeochemical sub-stepping. ROMS uses a split-explicit, semi-implicit time-stepping scheme (Shchepetkin and McWilliams, 2005). The 3-D baroclinic equations were integrated with Δt = 30 s, while the 2-D barotropic mode used 50 sub steps per baroclinic step (Δt_{fast} = 0.6 s). Vertical mixing/diffusion is treated implicitly for numerical stability, whereas advection and biogeochemical source–sink tendencies are updated on the baroclinic step."

The model has been evaluated coastwide (Renault et al., 2021, Deutsch et al., 2021) and more intensively within the SCB (Kessouri et al., 2021b, 2024) against observations of both ambient ocean state and rates, including hydrography, primary production, oxygen, carbonate chemistry, and chlorophyll-a. Across these scales, it reproduces the key observed gradients in physics, biogeochemistry and lower trophic ecosystem, including interannual variability and subregional patterns of diatom dominance in the Bight (Taylor and Landry, 2018, Kessouri et al., 2021b) and the influence of anthropogenic nutrient inputs on nitrogen and carbon cycling (Kessouri et al., 2021b).

2.2 Modeling approach

We applied the model to examine natural and anthropogenic drivers of diatom productivity and their influence on DA-producing HAB risk. A 20-year (1997–2017) simulation with all terrestrial inputs was investigated to characterize diatom productivity in the SCB and assess how processes such as upwelling and eddies, modulated by climate variability, affect diatom productivity.

To quantify natural versus anthropogenically enhanced diatom productivity and the risk of DA HABs, we assessed the difference between a control run excluding all terrestrial inputs (CTRL) with a scenario including all terrestrial inputs (ANTH) for 2013–2017. Early modeling studies identified the importance of terrestrial rather than atmospheric sources of nutrients in driving primary productivity in the SCB; treated wastewater nutrient inputs are three orders of magnitude larger than atmospheric deposition in this region (Howard et al., 2014). Sutula et al. (2021) provides a comprehensive description of the data representing terrestrial natural and anthropogenic sources to U.S. coastal waters from 19 municipal wastewater ocean outfalls and 75 rivers, representing the anthropogenic nutrient contributions of a coastal population of 23 million people. Constituents included fresh water, and total and dissolved inorganic and organic nitrogen, phosphorus, silicate, alkalinity, organic carbon and iron fluxes representing natural and anthropogenic sources from the coastal watersheds of the SCB that discharge to US coastal waters. Since less than 1% of riverine nutrient inputs are natural, 97% are point sources and 2% non-point sources (Sutula et al., 2021), increases in productivity between the ANTH and CTRL simulation are primarily anthropogenic in origin. Effluent discharges from Publicly Owned Treatment Plants (POTW) to ocean outfalls are strongly nitrogen-dominated: dissolved inorganic nitrogen (DIN) accounts for ~97% of the combined DIN + total inorganic phosphorus (TIP) mass released to the ocean (DIN: TIP ~ 30–40:1), indicating that most anthropogenic inputs are overwhelmingly nitrogen-rich. In addition, POTW-derived nitrogen is ~95-99% ammonium, a highly bioavailable form. POTW nitrogen loading is relatively steady through the year compared to rivers and stormwater, which exhibit strong wet-season pulses; consequently, seasonal variability in DIN loading is generally modest for outfalls but large for riverine sources.

In addition, we ran four modeling source attribution simulations to isolate contributions from U.S. permitted wastewater ocean outfalls and coastal rivers discharging directly to U.S. coastal waters, documented in Sutula et al. (2021), plus 2 additional wastewater outfalls that discharge primary or untreated sewage to Mexican beaches south of the U.S. border (Figure 1; Supplementary Table 1). The relative contribution of these sources is summarized in Table 1. Ocean outfalls represent 95% of the terrestrial nitrogen inputs, so the attribution experiments parsed their effects between (1) large POTWs that discharge > 100 million gallons per day (MGD) (+5–10^6 m^3 s^{-1}) to deep outfalls below the euphotic zone (50–98 m) versus (2) small POTWs)< 100 MGD) that typically discharge to shallow outfalls within the euphotic zone

TABLE 1 (A) Summary of the maximum cumulative days, the mean intensity above, the spatial footprint and the percent of the area of state and federal waters above the threshold of 3.3 mg m-3, operationally defined as the inflection point of increased risk of detecting DA above a probability of 0.5.

(A) Summary of the maximum cumulative day						
By Year	Mean intensity above threshold (mg Chl-a m^{-3})			Spatial Coverage (km^2)		
	CTRL	ANTH	Increment	CTRL	ANTH	Increment
Natural ocean	18,418			58%		
2013	6	19	13	16,707	26,741	10,034
2014	3	18	15	0	103	103
2015	4	20	16	186	611	424
2016	5	15	10	1,606	2,831	1,224
2017	5	17	12	3,715	5,807	2,092
(B) Relative contribution of risk of DA producing diatoms						
By Pathway	2013 Area (km^2) of Contribution to DA Risk (percent of SCB area)			Fraction contribution to total ANTH DA risk		
Natural ocean	18,418			58%		
U.S permitted deep outfalls (4)	7,062			22%		
U.S. permitted shallow outfalls (15)	2,639			8%		
Rivers discharging to US coastal waters (75)	1,748			5%		
Mexican beach outfalls (2)	1,677			5%		

The statistics are provided for natural variability (ocean only; CTRL scenario) versus anthropogenic enhanced (ANTH scenario), then the incremental increase (ANTH minus CTRL) by calendar year (2013 through 2017). (B) Relative contribution of risk of DA-producing diatoms from terrestrial pathways of anthropogenic nutrient inputs to the SCB domain for 2013. Incremental area is calculated via differencing source attribution scenarios (Table 2). Percent increase is calculated relative to the CTRL scenario (ocean only).

(< 50 m). Each of these source attribution scenarios was run for 17 months with 12 months (January–December 2013) used for analysis after the initial spin-up. To evaluate the impact of the various sources listed in Table 2, we subtracted each scenario from the control run (ocean only) to determine the cumulative footprints in each scenario.

ROMS-BEC predicts diatom biomass, so this variable could be explicitly pulled from the model outputs; investigations of the influence of anthropogenic nutrient inputs on the risk of DA HABs employed an observationally derived chlorophyll-a threshold of DA risk (Sandoval-Belmar et al., 2023), which was applied to ROMS-BEC predicted chlorophyll-a (detailed in Section 3.3.3).

TABLE 2 List of scenarios employed in study, by scientific question.

Study objectives	Scenario employed
1. Document the temporal and spatial variability of diatom productivity	• ANTH 1997 through 2017
2. Investigate the factors associated with natural versus anthropogenic forcing on diatom productivity: 1. Upwelling and eddies 2. Climate regime 3. Terrestrial (anthropogenic) inputs	Investigate oceanic factors: • ANTH 1997 through 2017 Investigate terrestrial (anthropogenic) factors via change assessment: • ANTH and CTRL, 2013 through 2017
3. Quantify how natural versus anthropogenic forcing modulate the window of opportunity for DA producing diatoms: ■ Document the spatial footprint and duration of the baseline (ocean only) risk? ■ Quantify the incremental risk due to terrestrial inputs? ■ Quantify the relative contribution to the incremental risk from various pathways of anthropogenic nutrient inputs	Apply operational definition of increased risk of DA detection when surface chlorophyll-a > 3.3 mg m^{-3} • CTRL 2013 to 2017 • ANTH 2013 to 2017 • U.S. deep ocean outfalls 2013 • All U.S. outfalls (deep plus shallow) 2013 • All outfalls plus rivers 2013 • ANTH plus Mexican beach municipal wastewater outfalls

ANTH refers to a scenario with full set of terrestrial inputs, which include all deep and shallow ocean municipal wastewater outfalls and rivers that discharge to U.S. coastal waters. CTRL refers to the scenario only with oceanic forcing and no land-based inputs. All outputs from these scenarios are stored at a daily averaged value for the full gridded resolution of the model domain.

2.3 Analytical methods

2.3.1 Temporal variability in diatom productivity

To characterize patterns in the temporal variability in diatom productivity, we decomposed the variability diatom biomass in the 20-year hindcast into distinct temporal scales, ranging from interannual to sub-seasonal. Vertically integrated diatom biomass, assessed between 0 and 100m, was extracted from the model output and averaged both daily and spatially over the entire domain. To investigate the dominant temporal variability modes, the total biomass signal was decomposed into four components using successive moving average filters: (1) interannual variability was isolated using a 365-day moving average filtered time series. (2) Seasonal variability was isolated with a 91-day moving average filtered time series minus a 365-day filtered time series. (3) sub-seasonal variability associated with mesoscale and submesoscale activity was isolated as the remaining unfiltered signal minus a 91-day filtered time series.

2.3.2 Investigation of oceanic physical processes, upwelling and eddies, the influence of anthropogenic nutrients, and modulation by climate regime

The southern CCS is nitrogen limited (Deutsch et al., 2021), so DIN availability in the euphotic layer is the principal determinant of primary productivity. Iron can also be seasonally limiting, particularly north of Point Conception, but in the SCB it is primarily supplied through natural sources rather than local human-derived inputs (Sutula et al., 2021).

To elucidate the impact of physical processes on DIN distribution within the euphotic layer, we employ a Reynolds decomposition technique utilizing a low-pass filter (Capet et al., 2008). Low-pass filters employ centered averages with 91-day windows to depict sub-seasonal variability. This variability is attributed to submesoscale and mesoscale circulation fluctuations, short-term upwelling events, and other frontal dynamics (Damien et al., 2024). The analysis is conducted at a fixed depth of 50 meters, which represents the average annual depth of the euphotic layer (Kessouri et al., 2020). $\overline{wN} = \overline{w'N'} + \bar{w}\bar{N}$, where w is the vertical velocity and N is the total concentration of DIN (nitrate plus ammonium).

Maps and time series of the vertical DIN flux were extracted to provide insights on drivers on diatom productivity during various climate cycles. For a more complete view of the mass-balance analysis, the approach used here has been published previously (Kessouri et al., 2024), and a brief description is provided in the Supplemental Information (SI). The years 1997 and 2017 were excluded from the statistics because the model did not cover those years entirely.

We use the Southern California Multivariate Ocean Climate Indicator (MOCI, García-Reyes and Sydeman, 2017), a composite climate index developed to capture regional oceanographic variability. It integrates multiple oceanographic variables such as sea surface and air temperature, sea level, and alongshore wind stress, atmospheric pressure and four climate indices (MEI [Multivariate ENSO Index], PDO, NPGO, NOI [Northern Oscillation Index]) into a single standardized metric, reflecting modulations caused by multiple atmospheric and oceanic climate cycles. Here, MOCI is used also to delineate years of positive and negative ENSO phases during surface temperatures and increased upwelling dominate the coastal and open ocean regions. These conditions enhance vertical mixing and shoal the nutricline, delivering nutrient-rich waters to the euphotic zone. ENSO phases are delineated in Figure 2, and an illustration of MOCI is presented in Supplementary Figure 13.

2.3.3 Linkage of diatom productivity to window of opportunity for DA-producing HABs

The basic premise of alteration of the window of opportunity of DA-producing PN blooms is predicated on the concept that factors that increase diatom productivity have the potential to elevate the biomass of DA-producing PN strains, which are consistently present and often dominant in the SCB (Barron et al., 2010; Umhau et al., 2018). Thus, if natural or anthropogenic factors increase the biomass of diatoms, then that widens the window of opportunity for DA-producing diatoms as well. Sandoval-Belmar et al. (2023) found a positive, significant correlation between chlorophyll-a (a bulk measure of total phytoplankton biomass) and the detection of pDA in ambient observations. In the central SCB, where greater than 60% of total DIN to the SCB is released, Sandoval-Belmar et al. (2023) identified a threshold of 3.3 Chl-a mg m^{-3}, above which the probability of DA detection exceeds 50%. DA detection is ecologically significant, since DA-related marine mammal strandings increase above baseline when DA is detected (Smith et al., 2023). This approach has been applied to investigate the effects of anthropogenic nutrient inputs on productivity and DA risk on the San Francisco and Monterey Coasts (Sandoval-Belmar et al., 2026). In the SCB, we assessed the skill of this approach by correlating the predicted annual areal risk of DA-producing HAB blooms (m^2) with the maximum annual observed particulate DA (pDA) concentration (mg DA m^{-3}) in the SCB from 2006 to 2017 (Smith et al., 2018).

This risk-based chlorophyll-a threshold was applied to ROMS-BEC predicted chlorophyll-a to identify the spatial footprint and duration of DA risk associated with the natural oceanic (CTRL) versus that impacted by anthropogenic nutrient inputs (ANTH) and to attribute the effect of specific source categories (i.e., U.S. deep outfalls, all US outfalls, all US outfalls and rivers, and finally all the sources including those from Mexican outfalls). Other factors can constrain DA production, so this modeled estimate is likely to estimate the upper range of areal DA risk.

A California Harmful Algae Risk Mapping (C-HARM) nowcast and forecast map predicts DA events based on an empirical formation that include remotely sensed chlorophyll-a (Anderson et al., 2016). While short-term fluctuations are critical for diatom blooms and the risk of DA events, multiple authors have noted that the key environmental drivers of annual primary productivity are typically present months before, effectively preconditioning the ocean for a subsequent spring bloom (Barron et al., 2010, 2013;

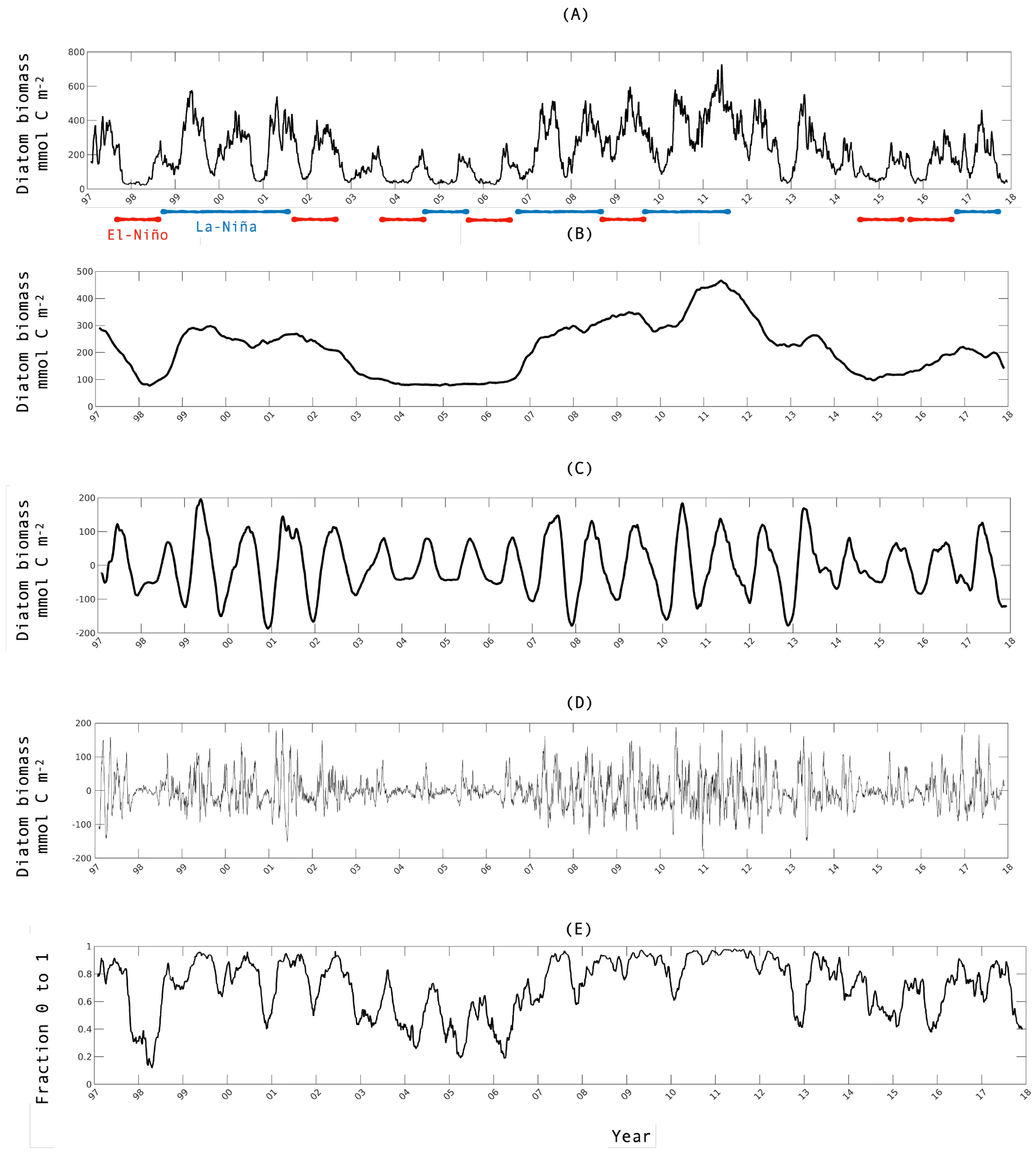

FIGURE 2
Time series of diatom biomass from 1997 through 2017 **(A)**, decomposed by component representing influences of different natural processes, from interannual variability due to climate regime **(B)**, CCS dominated seasonality **(C)**, sub-seasonal activity is an anomaly **(D)**. **(B–D)**, when combined, reconstruct **(A)**. And diatom fraction in Panel **(E)**. In **(A)**, the red and blue bars represent periods of El Niño or La Niña cycles.

Sekula-Wood et al., 2011). We used a similar approach to confirm the relative importance of different oceanic drivers in modeled DA areal risk, defined as the area exceeding > 3.3 mg Chl m^{-3}, using a stepwise regression model approach. Monthly averaged MOCI, upwelling intensity, eddy kinetic energy, and vertically integrated DIN in the epipelagic zone (0 to 200 m) were extracted from model output from October to April, then grouped into three-month running averaged intervals to test lags in stepwise regression models. These variables were regressed against the spatial extent of risk of DA HABs from January to December of the subsequent year. The October-December lag period was the most significant of any three-month period and was retained as the final temporal scale for the independent variables. Only the variables that demonstrated statistical significance ($p<0.05$) with no significant covariance were retained in the final model to predict modeled DA areal risk.

3 Results

3.1 Temporal and spatial variability

Diatom biomass in the SCB (Figure 2) varies across seasonal, sub-seasonal, and interannual timescales. Spring–summer blooms dominate the seasonal cycle, while interannual peaks occurred

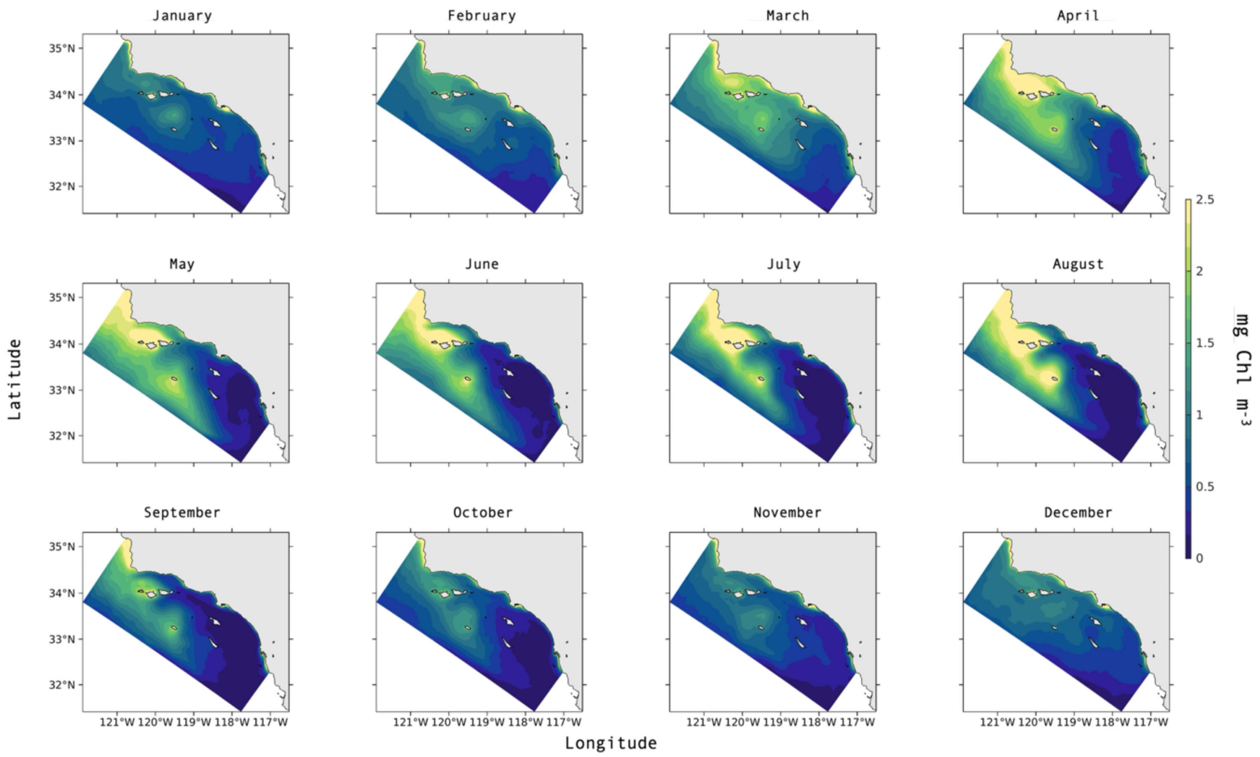

FIGURE 3
Spatial variability of 19-year averaged surface diatom concentration (mg Chl-a m^{-3}) predicted by ANTH, shown by month.

during 1999–2002 and 2007–2013 (Figure 2B). Reduced biomass and weaker variability characterized 2003–2006 and 2014–2016, when non-diatom groups were more prevalent (Figure 2E). Sub-seasonal processes, including mesoscale and submesoscale circulation, generate short-lived biomass pulses that can reach seasonal amplitudes (Figure 2D). These events, operating over weeks, are critical for bloom initiation, patchiness, and nutrient redistribution (examples of snapshots with various filters are available in Supplementary Figures 1 A–C). The period with less variability co-varies with most of the periods of lower diatom fraction, dominated by non-diatom groups.

Spatially, diatom concentration and productivity (Figure 3 with supported figure illustrating the integrated biomass Supplementary Figures S2) are heterogeneous (example of snapshot is provided in Supplementary Figures S1D). Although the continental shelf experiences strong winter–spring upwelling (annual mean 262 mmol C m^{-2}, maximum = 431 C mmol m^{-2}), the offshore domain, particularly around the Channel Islands, exhibits the highest annual and vertically integrated diatom biomass (annual mean = 371 mmol C m^{-2}, maximum = 636 C mmol m^{-2}). During summer, offshore biomass is ~40% greater than the coastal domain over the 0–200 m shelf.

3.2 Natural nutrient supply and climate forcing

Vertical DIN flux within the upper 50 m in the highlighted region in Figure 4A, the depth range supporting most natural phytoplankton productivity, shows strong interannual variability (Figure 4B). Between 2004 and 2011, the fluxes experienced a tripling. High-flux periods (1999–2002 and 2007–2013) were interspersed with low-flux years characterized by El Niño conditions (Figure 2A). During these low-flux years, horizontal export exhibited a relatively comparable intensity to vertical transport. Notably, the total horizontal flux was negligible in comparison to the vertical influx during the most La Niña years (Figure 4C). Wind stress curl significantly enhances vertical DIN flux (Figures 4D), explaining 44% of its variability ($r=0.66$, $p=0.01$, $n=20$, see Supplementary Figures S3). Notably, most El Niño years exhibit reduced wind stress curl during the preceding precondition seasons (Figure 4D and refer to Supplementary Figures 3, 4 for more detailed statistical information).

Total and Eddy-driven vertical nitrogen transport (Figure 5; see Supplementary Figures 5, 6 for the full list of years) peaks near the Channel Islands and Santa Cruz Basin (Figure 6A), intensifying during spring–summer (red bars in Figure 6B) and sustain blooms for up to 6 months. Figure 7 demonstrates the size and a cross section of those enriched mesoscale eddies (and see the movie in SI MS1 and associated physical conditions in Supplementary Figure 7). In contrast, shelf productivity is dominated by episodic wind-driven early spring (black bars in Figure 6B) upwelling events lasting <5 days, which rapidly elevate surface nitrate in narrow coastal bands (a demonstration of an upwelling event, with its associated physical conditions and its effects on DIN is presented in SI Supplementary Figure 8).

3.3 Anthropogenic enhancement of diatom productivity

Model simulations indicate that terrestrial nutrient inputs enhance vertically integrated DIN and diatom biomass relative to

10.3389/fmars.2026.1729816

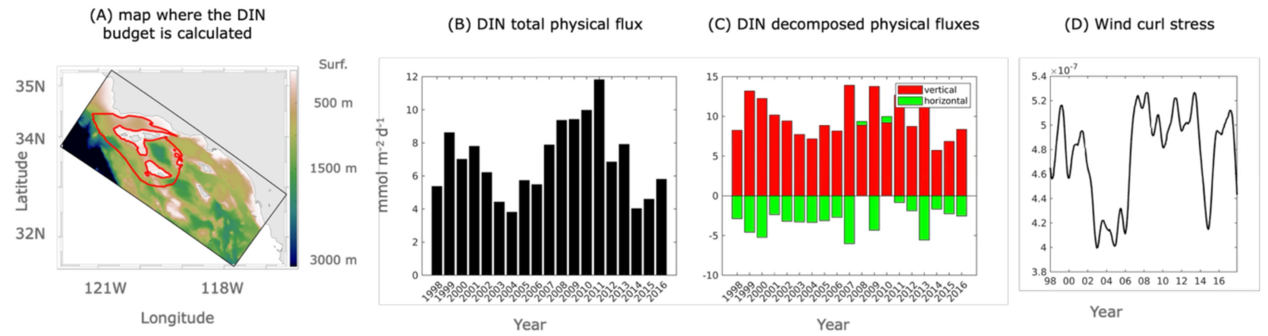

FIGURE 4
(A) Modeling domain is shown in the black box, color-coded background is bathymetry and red contour is the area where the analysis in B,C, and D is processed. **(B)** DIN total physical flux averaged per year. **(C)** Decomposed physical flux, vertical in red and horizontal in green, averaged per year. **(D)** Wind curl stress (N·m^{-3}) smoothed with a running mean and a window of 365 days. A measure of the rotational wind forcing over the ocean, shows interannual oscillations with peaks covarying with peaks in the vertical flux of DIN.

natural conditions. Enhancement is strongest near major urban outfalls and rivers in the central SCB but also extends offshore around Santa Catalina and the Channel Islands (Figures 8A, B). Effects are seasonally dependent, intensifying during summer and autumn. Between 2013 and 2017, mean biomass increased by 28.5 mmol C m^{-2}, with localized peaks exceeding 112 mmol C m^{-2}. In some years (e.g., 2017), biomass increased by up to 67% (Figures 8C, D). Additionally, offshore regions experienced stronger increases, particularly in a large region around and southeast of Santa Catalina Island and around the Channel Islands and San Nicholas Island, where the amplification was 5 mmol C m^{-2} on average and up to 29 mmol C m^{-2}. Moreover, the amplification was greater in summer and autumn, where it reached 8 and 45 mmol C m^{-2} respectively on average, and up to 24 and 81 mmol C m^{-2}.

Climate modulates anthropogenic influence. Figure 9 shows an example at an outfall in Santa Monica Bay during two antagonistic years (the complete list of years is shown in SI Supplementary Figure 9). During El Niño, deepened stratification limits vertical nutrient supply and isolates nearshore urban outfalls plumes, particularly along San Pedro shelf and the Los Angeles area. During La Niña, a shoaled nutricline facilitates broader nutrient delivery through upwelling and eddies, amplifying both natural and

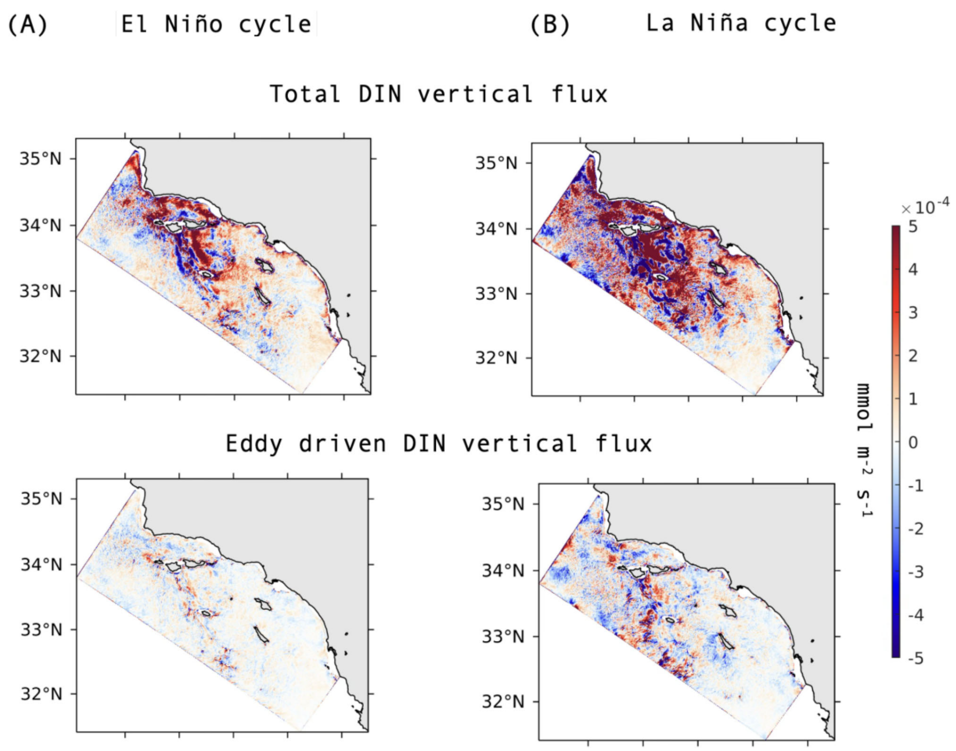

FIGURE 5
Color-coded maps illustrating spatial heterogeneity in the DIN vertical total (top panels) and $w'N'$ flux filtered with Reynolds decomposition using a 91-day filter (bottom panels) at 50m depth (mmol m^{-2} s^{-1}), averaged in **(A)** 1998 (to reflect El Niño cycle) and **(B)** 2008 (to reflect La Niña cycle). Annual averages across the 19 years of model simulation are presented in Supplementary Figures S13, S14.

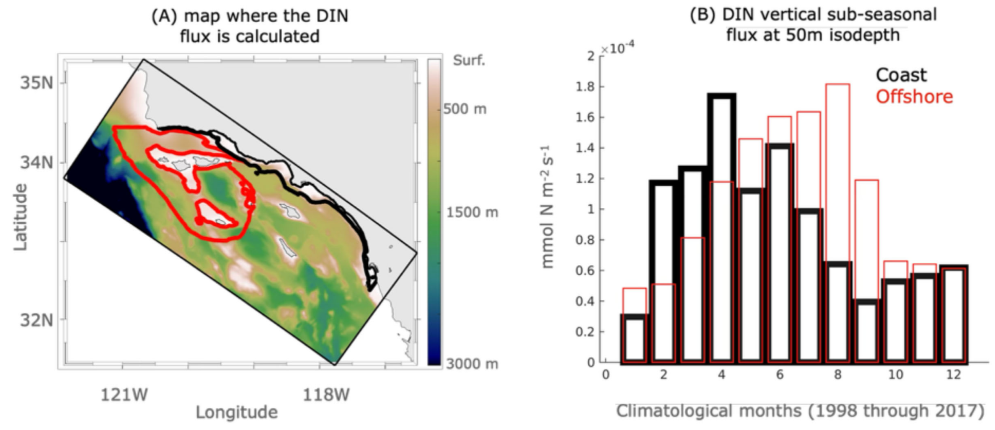

FIGURE 6
(A) Map of the region with coastal (black outline) and offshore (red outline) domains. **(B)** Monthly climatology of DIN flux at 50 m isobath from 1998–2017, showing coastal (black) and offshore (red) variability.

anthropogenic signals. This pattern results from intensified shoaling of the nutricline (Figure 9), facilitating the delivery of nitrate and ammonium into the euphotic zone.

3.4 Implications for DA-producing HAB risk

The CTRL (natural ocean) simulation indicates that in 2013, an intermediate productivity year, the naturally occurring area at risk of DA-producing HABs (> 3.3 mg Chl m^{-3}) was 16,707 km^2 (Table 1), concentrated in the Santa Barbara Channel, north of Point Conception, around the Channel Islands, and in persistent offshore eddies (not shown). Bloom severity above the risk threshold was low (+6 mg Chl m^{-3}), and southern Santa Barbara Channel and central/southern SCB nearshore waters rarely exceeded the threshold. Other years (2013–2017) were lower productivity, with the chlorophyll-a threshold exceeded less frequently than in 2013 (Table 1).

Anthropogenic nutrient inputs increased the magnitude, spatial footprint, and duration of DA risk, with year-to-year variability (Table 1). In 2013, the footprint expanded by 60% (10,034 km^2), the duration increased by ~5 months, and severity rose by +19 Chl mg m^{-3} above the base threshold of 3 mg m^{-3} (Table 1), with expansion in state and federal waters (annual comparison of the effects on the CA state versus US federal waters are presented in SI Figure 10). The strongest effects occurred in coastal Orange County, Los Angeles, and Ventura regions where the CTRL predicted little prior risk. Risk area and duration increased during winter/spring (December–May) and autumn (September–November; Figures 10A, B), with offshore duration increases up to 70 days near the Channel Islands (Figure 10C). Seasonal productivity changes were greatest in the Central and North SCB coastal band in winter–spring (Figures 10B, C) and offshore in summer–autumn.

Source attribution shows deep and shallow outfalls in the Central SCB contributed most to increased 2013 risk. Table 1

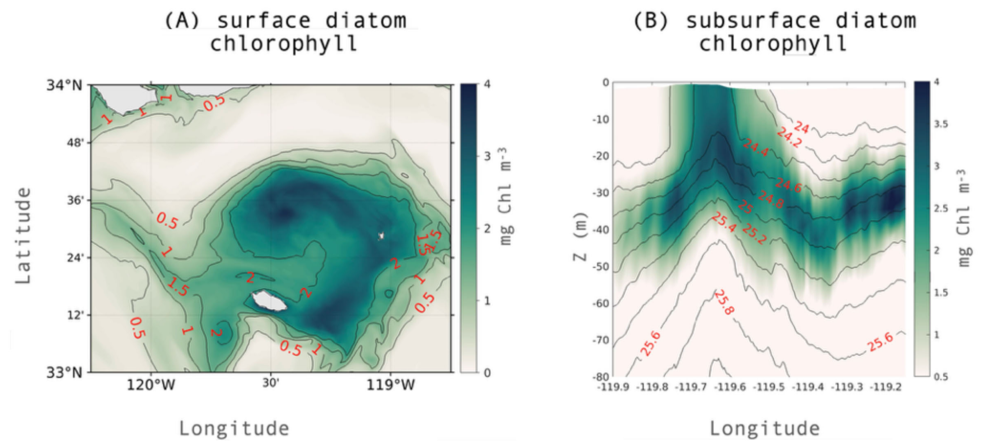

FIGURE 7
A visual representation of the influence of a substantial, enduring cyclonic mesoscale eddy on the augmentation of diatom biomass is depicted. **(A)** showcases a color-coded background and contours, both of which indicate surface diatom concentration in milligrams of chlorophyll per cubic meter (mg Chl m^{-3}) over a mesoscale eddy generated within the Santa Cruz deep Basin. **(B)** presents a cross-sectional perspective of the eddy depicted in **(A)**, with the background illustrating diatom chlorophyll concentration and contours denoting relative ocean potential density.

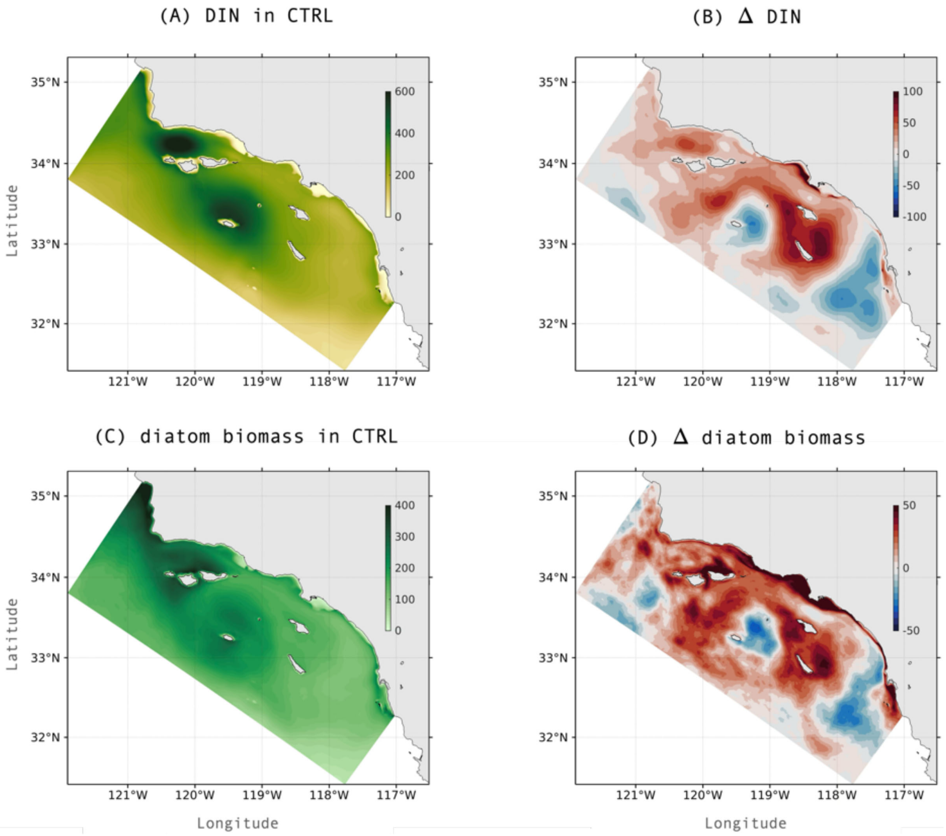

FIGURE 8
Modeled change in vertically integrated DIN and diatom biomass (mmol C m^{-2}) in the SCB due to anthropogenic nutrient inputs from continental sources, as simulated by the ROMS-BEC model and averaged over 2013–2017. The figure shows the vertically integrated DIN in the natural ocean **(A)** versus the change in DIN [**(B)**, ANTH minus CTRL] and diatom biomass in the natural ocean **(C)** versus the change in diatom biomass [**(D)**, ANTH minus CTRL] due to the addition of anthropogenically-enhanced terrestrial nutrients. .

quantifies pathway-specific expansion relative to CTRL, and Figure 11 shows the approximate (order-dependent) footprint. Deep outfall effects extended from mid-Orange County to the central Santa Barbara Channel and offshore around the Channel Islands (Figure 12). Rivers and shallow outfalls expanded risk northward as well as in nearshore and eddy regions. Mexican beach outfalls contributed 5% above the natural areal extent of the SCB but were locally significant south of San Diego Bay (Figure 12).

Of the five years analyzed, 2013 was most productive; 2014–2016 showed low or near-zero risk. In 2017, natural risk was low but anthropogenic inputs doubled the spatial footprint and increased intensity to 13 mg m^{-3} above the threshold (Table 1), with proportionally larger effects than 2013 (maps of annual change in

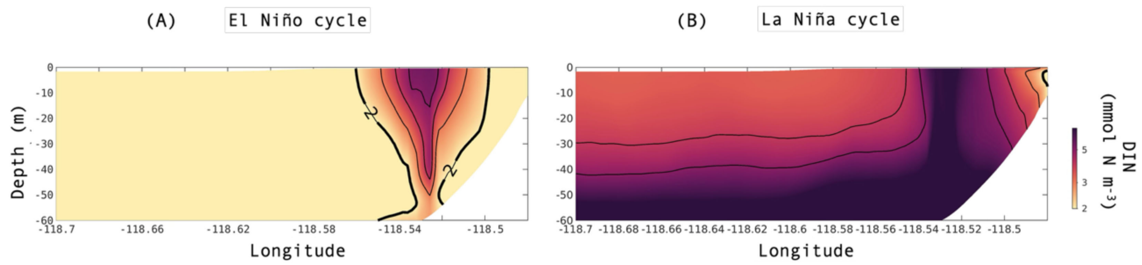

FIGURE 9
These figures, color-coded backgrounds and contours, depict the total DIN concentration in mmol nitrogen per m^3 across vertical cross sections of Santa Monica Bay, situated near the City of Los Angeles Hyperion outfall. The right side of the image represents the coastline, while the outfall is located at the bottom, where the plume is situated. These figures illustrate the modulation of anthropogenically enhanced nutrient sources at ocean outfalls by climate regimes during the El Niño 1998 **(A)** and La Niña 2008 **(B)** cycles.

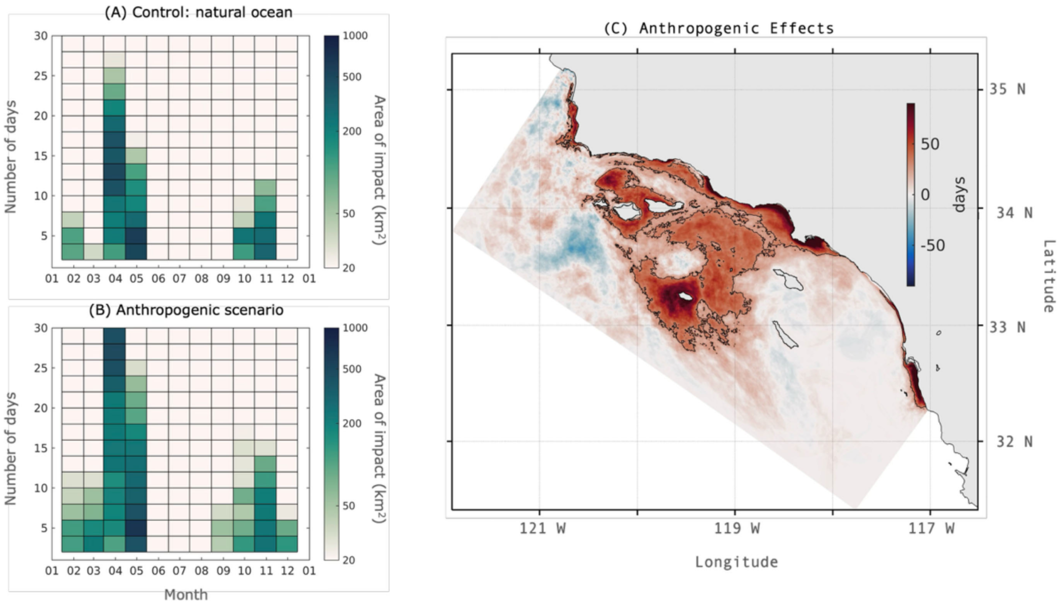

FIGURE 10
Left Panels: Temporal change in the probability of DA detection greater than 50% (Chl-a > 3.3 mg m^{-3}) by month (X axis) and number of days per month (Y axis), scaled to a color bar of the area of impact (km^2), where deeper green indicates greater area. **(A)** is the natural ocean and **(B)** is the ANTH simulation showing the additionality of terrestrial nutrients. **(C)** shows the increased in the spatial footprint of DA risk due to anthropogenic nutrients with the heat map defined in the increase of risk days in the SCB. Black contour is percentile 25.

risk of HABs are presented in SI Supplementary Figure 11). Although the most productive year in 2013–2017, 2013 was moderate relative to the past two decades; years such as 1999, 2009, 2010, and 2011 showed Bight-wide DA risk expansion (maps of annual change in risk of HABs in ANTH run is presented in SI Supplementary Figure 12).

3.5 Predictors of interannual DA risk

The predicted areal DA risk varied significantly on an interannual basis (Figures 11A, B). Peak risk periods occurred in 1999, 2009, 2010 and 2011, with dampened risk during the more

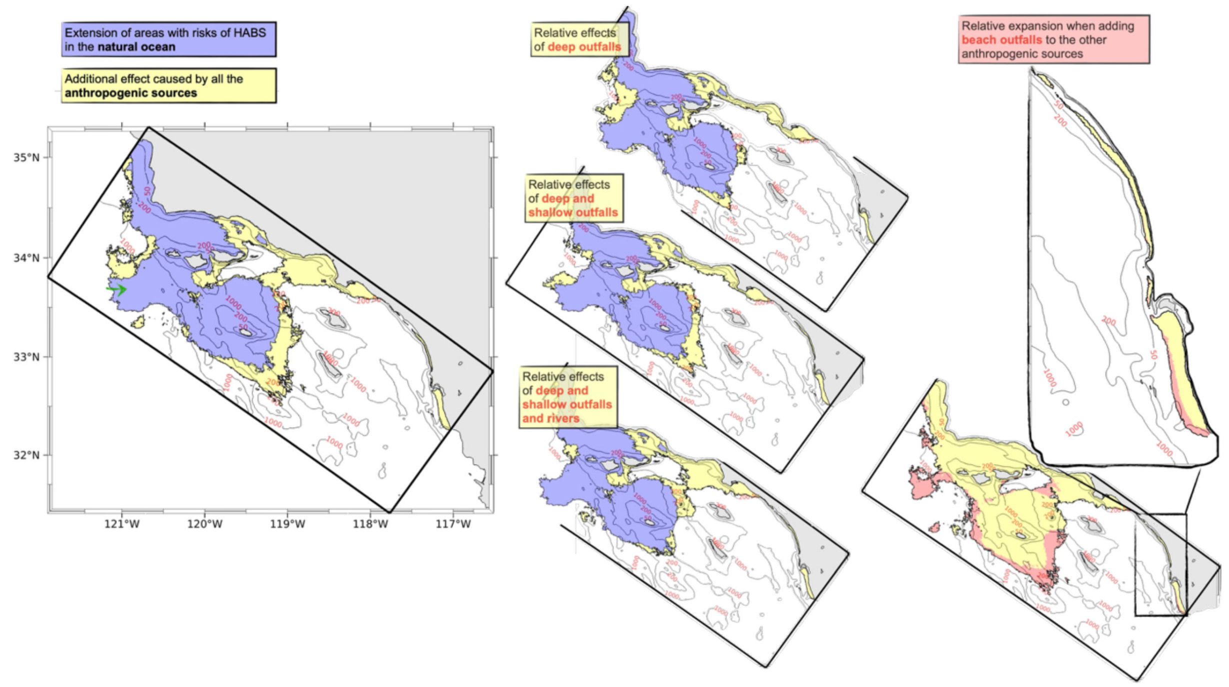

FIGURE 11
Predicted relative additional contribution of terrestrial nutrient pathways to spatial footprint of elevated HAB risk above natural variability (ocean only, purple), and additionality due to US deep outfalls, US shallow outfalls, US and Tijuana Rivers draining to US coastal waters (yellow), then from beachoutfalls discharging to Mexican coastal water (red shadow). The maps distinguish between zones where such conditions occur under naturaloceanic conditions (purple) and areas where they arise due to anthropogenic nutrient inputs. The black bounding box outlines the model domain.

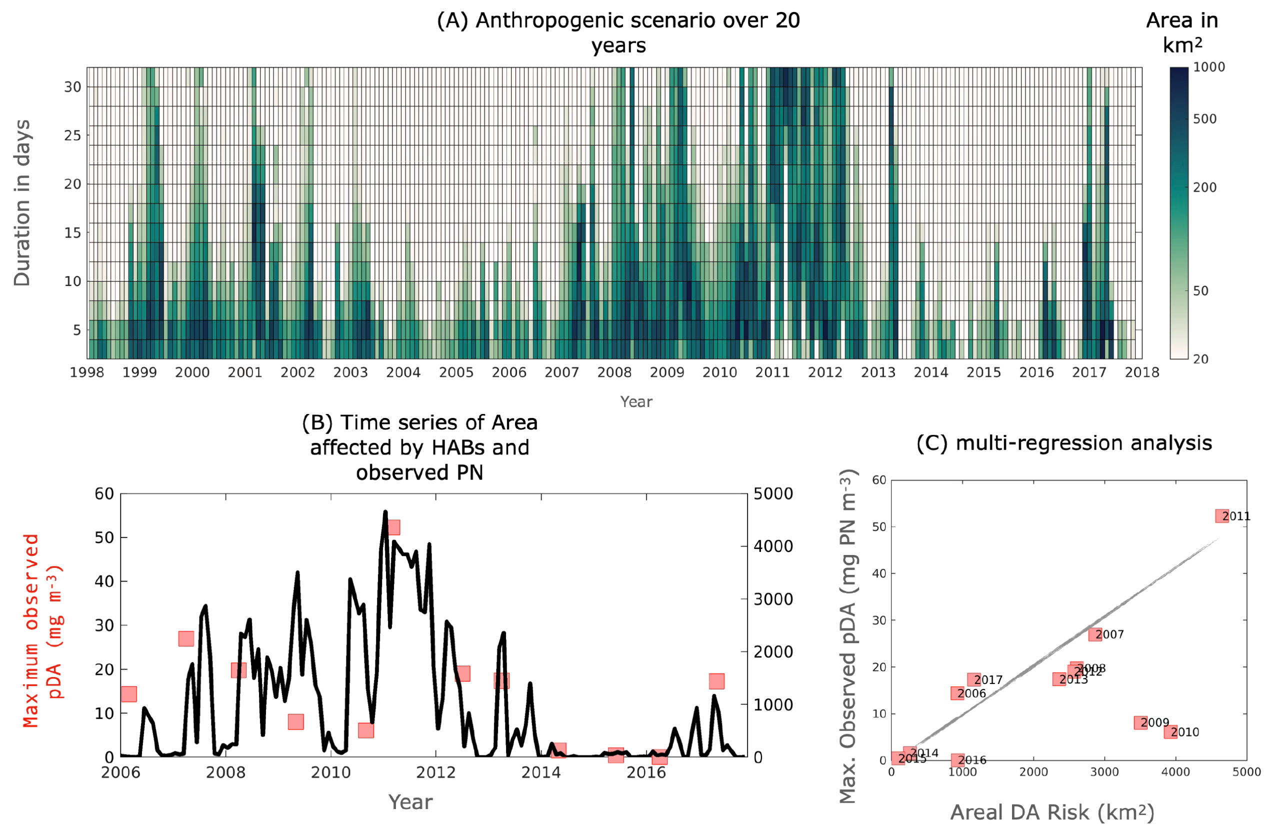

FIGURE 12
(A): area (km^2)and duration (days) of DA risk in ANTH scenario over a 20 year period, from 1998 to 2017. **(B)**: Annual maximum observed particulate domoic acid (mg DA m^{-3}) (left Y axis, red squares) superimposed on time series of Bight wide simulated areal DA risk (km^2), i.e. > 3.3 mg Chl m^{-3}) over 2006 through 2017. **(C)** regression of maximum annual observed DA concentrations versus predicted areal DA risk. Years included in the analysis in **(B, C)** are those with available observation of particulate DA and therefore do not include the full 20 year ROMS-BEC simulation.

recent period of 2014-2016. A scatter plot (Figure 11C) of maximum pDA concentrations (mg DA m^{-3}) with this predicted areal DA risk (m^2) shows a strong correlation (R = 0.75, p-value<0.01), providing an independent confirmation of the utility of a screening chlorophyll-a threshold in combination with ROMS-BEC predicted chlorophyll-a to predict annual DA areal risk.

We further investigated this stepwise regression to identify which environmental drivers were most predictive of areal DA risk. Two independent variables were retained and thus appear to strongly precondition the SCB for high diatom productivity and areal DA risk: MOCI (Supplementary Figures S13) and vertically integrated DIN. The multiple regression model was highly predictive (F = 45.75, p < 0.0001, RMSE = 550.5 km^2, R^2 of 0.85), with 55% of the interannual variance in area explained by MOCI and 45% vertically integrated DIN.

4 Discussion

This study illustrates the power of a validated, regional ocean numerical model to investigate the processes driving the diatom productivity in the SCB. These underlying key processes potentially contribute to blooms of *Pseudo-nitzschia* spp., a pennate diatom commonly found in the SCB, and therefore increased risk of events of its toxin DA. In this region that has some of the highest DA concentrations documented in the literature (Smith et al., 2018), observational syntheses have previously highlighted the role of large-scale climate variability, upwelling, and sources of anthropogenic nutrients such as ocean outfalls and rivers (Sandoval-Belmar et al., 2023; 2026; Smith et al., 2018) on DA events. Our modeling analysis confirms the importance of these drivers on the SCB but provides a substantially more nuanced view of their subregional influence. Furthermore, we attribute natural versus anthropogenic drivers, including specific anthropogenic sources, that are predicted to elevate the probability of detecting DA producing PN blooms in time and space. Thus, ROMS-BEC, a well-vetted biogeochemical model of known skill (Kessouri et al., 2021b; 2024, National Water Research Institute, 2024) can play an early role in shaping scientific understanding and screening potential HAB mitigation strategies, while efforts to refine and apply a recently developed DA mechanistic model are ongoing (Moreno et al., 2022; Sandoval-Belmar et al., 2026).

4.1 Significance of natural oceanic versus anthropogenic drivers of diatom productivity, modulated by large-scale climate variability

This study highlights the highly dynamic nature of upwelling, eddies, and turbulence, modulated by large-scale climate variability, and amplified by urban eutrophication in driving the oceanic variability of diatom productivity. Shelf wind driven upwelling (García-Reyes and Largier, 2012; Kahru et al., 2018), geostrophic adjustment within the SCB (Mantyla et al., 2008), eddies (Dong et al., 2009; Dong and McWilliams, 2007), and wintertime surface mixing and densification all modulate mixed layer depth and the isopycnal shoaling that delivers deep pools of DIN to the photic zone. While upwelling and its associated circulations and instabilities are often the most cited factor driving natural productivity in the CCS (Mantyla et al., 2008), recurring coastal and offshore mesoscale eddies appear also to play a crucial role in sustaining the SCB diatom production. In the presence of islands, these eddies can be generated by the phenomenon known as island mass effects (Kessouri et al., 2022). These eddies play four pivotal roles: (1) they facilitate the transport of nutrients to the surface, (2) they ensure the persistence of these nutrients, sustaining active nutrient delivery and diatom productivity for multiple months from spring to autumn, (3) they export coastal nutrients from shelf upwelling, from the northern region, and from anthropogenic coastal sources such as outfalls and rivers (Kessouri et al., 2024), and (4) they trap and retain nutrients and organic matter originating from coastal eutrophication in the offshore domain for multiple months after their export (Kessouri et al., 2024).

Multiple studies have demonstrated how primary productivity and surface chlorophyll-a have varied over the past decades and how climate cycles have influenced periods of El Niño, productive La Niña, and warming events (i.e. blobs). However, most of these studies have relied on observational data that are either sparse or not temporally resolved (Nezlin et al., 2018; Thomas et al., 2013) or broad-scale, lower resolution models (Deutsch et al., 2021). Our high resolution, 20-year ANTH hindcast captures the range of large-scale climate oscillations, including ENSO, PDO, and heatwaves (McGregor, 2024), which modulated the physical processes controlling diatom productivity via wind stress, eddies, upwelling, stratification, and the depth of the nutricline (Kahru et al., 2018). During negative MOCI phases diatom biomass exhibits a substantial expansion, primarily attributed to the favorable nutrient availability, promoting seasonal blooms that dominate primary productivity (Lavaniegos et al., 2002; Thompson et al., 2024). Coastal eddy activity is amplified under enhanced alongshore wind stress curl, facilitating both vertical and lateral nutrient transport and further supporting productivity over broader shelf regions. In contrast, during positive MOCI (corresponding to El Niño conditions, above average precipitation and warm temperatures), stratification and deep nutriclines occur. Hence, seasonal expansion of diatom biomass is reduced, and the eddy activity and its biological modulation is also diminished (Gómez-Ocampo et al., 2018).

Anthropogenic nutrient inputs act to enhance this natural diatom productivity, particularly nearshore proximal to wastewater and riverine sources and in locations of persistent offshore eddies. The majority of terrestrial inputs are discharged to ocean outfalls, so the anthropogenic subsidy is largely chronic (Sutula et al., 2021). These inputs act to enhance vertically integrated DIN within the photic zone, a variable linked to diatom productivity, which can act to precondition the water column for diatoms that include DA-producing PN HABs. Over the period of 2013 to 2017, these inputs enhance diatom productivity by 20% on the coastal shelves, with less effect offshore. The effect of these anthropogenic nutrient inputs to the SCB coastal productivity has previously been reported (Kessouri et al., 2021a; 2024), but the focus of these explorations has been on enhanced respiration, oxygen and pH loss, and their seasonal effects on the compression of pelagic aerobic and calcifiers habitat (Frieder et al., 2024), rather than on the risk of DA-producing HABs.

4.2 Evidence of linkage of diatom productivity to risk of DA-producing HABs

Previous authors have noted the considerable interannual variability of DA events, with 2003, 2006, 2007, 2011, and 2017 notable for the importance of these events to marine mammal and seabird mass strandings and mortality (Smith et al., 2018). We found the MOCI index and vertically integrated DIN together predicted 85% of interannual variability in areal DA risk, and this areal risk was significantly positively correlated to maximum pDA. The strength of the sub-seasonal dynamics, such as eddies and local wind-driven shelf upwelling, and anthropogenic nutrient inputs further enhanced surface DIN pools, on top of a natural oceanic baseline (Kessouri et al., 2021a, 2024). Climate variability strongly modulates the shoaling of DIN-rich waters via controls on the underlying physical processes (Gómez-Ocampo et al., 2018). Not all high DA years were correctly predicted (2009, 2010). It is unclear whether field observations failed to capture a PN bloom, but we must also point to the limitation of using predictions of diatoms alone in lieu of a more advanced model (e.g. Moreno et al., 2022; Sandoval-Belmar et al., 2026) that can mechanistically enhance or constrain DA production based on intrinsic factors that can further promote or moderate DA cellular toxin production (e.g. silicic acid limitation; Sandoval-Belmar et al., 2023; Bates et al., 2018). The relative error in this spatial DA risk estimate (RMSE of 550 km^2) was low during moderate to high productivity years (< 5%) and understandably high (e.g. > 20%) during low productivity years (when non-diatoms dominate). Autumnal oceanic conditions appear to precondition the SCB coastal ocean, making it more susceptible to DA events, a finding that has importance for seasonal predictability that could be beneficial to inform DA event response (see section on management implications), but more work is needed to predict the location (inshore/offshore), timing and duration of DA events.

4.3 Role of anthropogenic nutrients in widening the window of opportunity for DA-producing HABs

Using an operationally defined risk threshold of 3.3 mg m^{-3} associated with 50% probability of detecting DA (Sandoval-Belmar et al., 2023), we found that the natural ocean without anthropogenic nutrient inputs has an inherent, quantifiable risk for the occurrence of DA events. This risk was greatest in previously well documented hotspots, including the Northern Santa Barbara Channel, around the Channel Islands, and north of Point Conception (Anderson et al., 2006; Smith et al., 2018). In 2013, we found the footprint of this region to extend over 16,000 km ^{2}, but the risk was of shorter duration and low intensity, with predicted values up to +5 mg m^{-3} above the DA risk threshold. The year 2013 is considered a moderate diatom productivity year. However, the "ocean only" CTRL simulation does not extend to periods of peak diatom production (2009-2012), and extending the simulation to cover those years would provide a more complete context of natural background variability in DA risk.

Anthropogenic nutrient inputs are predicted to widen the window of opportunity for DA-producing diatoms by intensifying the severity of the DA risk, extending the spatial footprint (inshore and offshore), and the seasonal window. Multiple types of observational data support these risk predictions. Our risk analyses suggested an amplification of DA events in northern Orange County through the southern Santa Barbara Channel, a location where the ocean-only CTRL scenario would predict that DA events would be rare. The San Pedro and Santa Monica Bays are locations with some of the highest surface water DA values recorded (Smith et al., 2018) and a hotspot in sediment DA (Sekula-Wood et al., 2009; Smith et al., 2021), relative to regions with less anthropogenic nitrogen inputs (south Orange and northern San Diego counties). An analysis of sediment cores in the Santa Barbara Basin revealed increased abundances of *P. australis* beginning in the early 1980s through current day (Barron et al., 2010), corresponding to the timeframe when the Southern California coastal human population doubled (Sutula et al., 2021). Predictions of increased intensity, duration and footprint of DA events are ecologically relevant for marine mammal and seabird illness and death, as they cannot avoid the DA that bioaccumulates in fish and benthic invertebrates that serve as their principal food source (Smith et al., 2023).

Previous modeling analysis has shown that primary production, which is diatom dominated, is proportional to DIN loading (Ho et al., 2023). For this reason, in our source attribution assessment of DA risk (outfalls, rivers, etc.) we found that DA risk was roughly proportional to the amount of loading, with large deep outfalls representing the largest contribution, followed by small shallow outfalls, while rivers and Mexican beach outfalls were roughly equivalent. However, we note that sources that discharge to the shallow photic zone, whether ocean or beach outfalls or rivers had a disproportionately higher response, because they are more immediately available to support primary productivity (Kessouri et al., 2024). Depth of discharge matters, but also the form of nitrogen. BEC modeled uptake rates for ammonium are higher than for nitrate (Hoel et al., 2024). Moreover, previous studies have shown that many PN species can effectively utilize ammonium nitrogen forms for growth and toxin production (Howard et al., 2007; Radan and Cochlan, 2018; Thessen et al., 2009).

Climate oscillations modulated the importance of anthropogenic nutrients in supporting diatom vs. non-diatom dominated productivity, which has relevant consequences for both DA-producing diatoms and non-diatom HABs. Of particular importance is the fate of deep outfalls wastewater plumes, which represent about 80% of total anthropogenic inputs (Kessouri et al., 2021; 2024). During La Niña years, these plumes add to the natural oceanic supplies of nitrate and silicate, enhancing diatom productivity both locally and offshore over remote areas across the SCB. Seegers et al. (2015) found significant outbreak and surface manifestation of the PN blooms coinciding with periods of upwelling, or other processes that caused shoaling of the pycnocline and subsurface chlorophyll maximum. They highlighted that populations of PN in chlorophyll-a maxima around wastewater plumes can be important "seeding" for surface PN blooms. During low productivity El Niño years, when the deeper, oceanic nutricline is isolated from surface waters, ammonium-enriched wastewater plumes from shallow and deep outfalls are the dominant source of nutrients available to support productivity in coastal zones. Inshore PN blooms that occur during these years are likely largely supported by anthropogenic nutrients. Our modeling analysis demonstrates that those periods (2016/2017, 2020), and by extrapolation more recent warmer years, tend to be dominated by small phytoplankton (i.e. non-diatoms), including multiple dinoflagellate HABs species (e.g., red tides). These species have the ability to vertically migrate to access deep pools of nitrate (Zheng et al., 2023), lasting for periods from two to six weeks, and can occasionally cause hypoxic events and fish kills (Skelton et al., 2024). Our model has limited ability to predict the dynamics of other phytoplankton groups during non-diatom dominated years; further work is needed to adequately describe model capability during these periods.

4.4 Modeling uncertainties and future directions

Multiple sources of uncertainty exist in our analyses. One potential source is the degree to which ROMS-BEC can adequately predict diatom productivity, as measured in chlorophyll-a. Model skill assessments have demonstrated that ROMS-BE adeptly captures horizontal and vertical gradients in remotely-sensed and ship-based primary productivity and chlorophyll-a in the SCB (Kessouri et al., 2021), lending credibility to model use for this application.

We also acknowledge that our simple DA risk prediction paradigm only considers the controls on diatom production. HABMAP data documents chlorophyll-a observations that are not associated with DA events, suggesting dominance of non-DA producing taxa (Sandoval-Belmar et al., 2023). Indeed, cell counts of large size-class PN cells have been identified as a more reliable predictor of DA events than chlorophyll-a (Seubert et al., 2013). Although PN cell abundance could yield a much tighter relationship with DA events, these observations are often rare relative to chlorophyll-a, and mostly at pier stations. PN cell abundance is also an imperfect predictor of pDA concentration because toxin production depends on the PN species in a bloom and their physiological state, which are not easily resolved by microscopy, and thus rarely characterized (Smith et al., 2018). Other factors, such as algal interspecies competition, top-down grazing, temperature constraints, nutrient and iron imbalances can act to further constrain this "window" in which DA events occur (Anderson et al., 2008; Brunson et al., 2024; McKibben et al., 2017; Sandoval-Belmar et al., 2023) but are not explicitly considered in this simple risk characterization. The range of risk threshold identified by Sandoval-Belmar et al. (2023) ranged from 1.8 mg m^{-3} in the Santa Barbara Channel to 3.3 mg m^{-3} in San Pedro Bay. The Sandoval-Belmar et al. (2023) did not produce a threshold specific to San Diego, so there is greater uncertainty in our estimates of risk for that region. These subregional considerations are likely to alter the footprint, intensity and duration of DA risk, but would not alter the fundamental conclusion that anthropogenic nutrients are modifying DA risk.

Uncertainty exists in the source attribution analyses. Natural sources of nutrients include terrestrial runoff from natural lands and are included in our estimates of river runoff. However, while they only represent < 1% of the terrestrial loads to the SCB, they are not specifically in our CTRL scenario. Uncertainty also exists in the exact locale of the spatial footprint of these individual source clusters, especially of smaller sources, because of model stochasticity in predictions of eddies and high frequency turbulence. Increased confidence in these findings could be achieved by extending the model simulations to longer time periods and repeating the source attribution experiments by progressively removing sources in a different sequence, to help constrain the uncertainty in the spatial footprint of effect.

Assessing the risk of particulate DA occurrence with this simplified modeling is an important advance, but more focus needs to occur using more advanced models that can mechanistically constrain the factors that modulate the production of DA. That work, based on the approach of Moreno et al. (2022) is in the early stages in the SCB, but with findings that point to model skill in predicting DA and its fate in the marine environment (Sandoval-Belmar et al., 2026). However, the link to DA-related shellfish advisories and marine mammal stranding is an important one and remains poorly understood (Smith et al., 2023).

4.5 Management implications

These findings highlight the value of utilizing validated biogeochemical models alongside emerging mechanistic HAB models (Sandoval-Belmar et al., 2026) into regional studies designed to support decisions aimed at reducing the impacts of HABs on coastal ecosystems. The management implications of our DA HAB modeling work fall into categories of (1) HAB prevention, focused on addressing underlying drivers to reduce the likelihood or severity of blooms (e.g., reduction in anthropogenic nutrients) and (2) HAB mitigation strategies to reduce the impact, once the bloom has occurred (Smith et al., 2026).

In the SCB, regional water quality managers have already been discussing the merits of nutrient nonpoint source control and wastewater-treatment-plant upgrades to address urban eutrophication effects on acidification and hypoxia (National Water Research Institute, 2024). With this study, we have demonstrated that ROMS-BEC predictions of areal DA risk could be considered as a screening level assessment alongside predictions of habitat compression of acidification and hypoxia (e.g. Frieder et al., 2024) to support those ongoing management discussions, while mechanistic DA modeling is advancing (Sandoval-Belmar et al., 2026). Ultimately, model refinements, improved monitoring, and additional model simulations representing realistic nutrient management scenarios are needed to inform those strategies as well as future applications to forecast the evolution of DA risk with climate change.

While prevention is a critical component of HAB management, these management actions take significant time and economic investments to implement; short-term strategies are needed to mitigate the impact once a bloom has occurred, such as efficient event response. The California Harmful Algae Risk Mapping model (C-HARM) is an operational forecast model that uses a combination of numerical ocean models, satellite data, and statistical models to generate daily forecasts of PN blooms and DA events (Anderson et al., 2016). Knowledge of an autumnal preconditioning may help to expand C-HARM to seasonal forecasts, allowing local organizations involved in marine mammal stranding and public health protection with a longer lead time to garner resources (Smith et al., 2021).

Data availability statement

The datasets presented in this study can be found in online repositories. The names of the repository/repositories and accession number(s) can be found below: https://zenodo.org/records/4448224.

Author contributions

FK: Conceptualization, Data curation, Formal Analysis, Investigation, Methodology, Software, Supervision, Validation, Visualization, Writing – original draft, Writing – review & editing. MS: Conceptualization, Data curation, Funding acquisition, Methodology, Resources, Supervision, Writing – review & editing, Writing – original draft. JS: Conceptualization, Data curation, Investigation, Methodology, Validation, Writing – review & editing, Writing – original draft. JM: Conceptualization, Investigation, Methodology, Software, Supervision, Writing – review & editing. MS-B: Conceptualization, Investigation, Methodology, Writing – review & editing. DB: Conceptualization, Funding acquisition, Investigation, Methodology, Project administration, Resources, Software, Supervision, Validation, Writing – review & editing. PD: Conceptualization, Methodology, Writing – review & editing. MH: Data curation, Methodology, Validation, Writing – review & editing. RK: Conceptualization, Methodology, Supervision, Validation, Writing – review & editing. CA: Conceptualization, Funding acquisition, Investigation, Methodology, Resources, Supervision, Validation, Writing – review & editing.

Funding

The author(s) declared that financial support was received for this work and/or its publication. This research was supported by NOAA grant NA18NOS4780174 and California Ocean Protection Council grant C0831014. This work used the Expanse system at the San Diego Supercomputer Center through allocation TG-OCE170017 from the Advanced Cyber infrastructure Coordination Ecosystem: Services and Support (ACCESS) program, which is supported by National Science Foundation grants 2138259, 2138286, 2138307, 2137603, and 2138296.

Acknowledgments

Additional computational support was provided by UCLA's Hoffman2 Shared Cluster, maintained by UCLA Office of Advanced Research Computing's Research Technology Group.

Conflict of interest

The author(s) declared that this work was conducted in the absence of any commercial or financial relationships that could be construed as a potential conflict of interest.

Generative AI statement

The author(s) declared that generative AI was not used in the creation of this manuscript.

Any alternative text (alt text) provided alongside figures in this article has been generated by Frontiers with the support of artificial intelligence and reasonable efforts have been made to ensure accuracy, including review by the authors wherever possible. If you identify any issues, please contact us.

Publisher's note

All claims expressed in this article are solely those of the authors and do not necessarily represent those of their affiliated organizations, or those of the publisher, the editors and the reviewers. Any product that may be evaluated in this article, or claim that may be made by its manufacturer, is not guaranteed or endorsed by the publisher.

Supplementary material

The Supplementary Material for this article can be found online at: https://www.frontiersin.org/articles/10.3389/fmars.2026.1729816/full#supplementary-material

References

Anderson, C., Brzezinski, M., Washburn, L., and Kudela, R. (2006). Circulation and environmental conditions during a toxigenic Pseudo-nitzschia australis bloom in the Santa Barbara Channel, California. *Mar. Ecol. Prog. Ser.* 327, 119–133. doi: 10.3354/meps327119

Anderson, C. R., Kudela, R. M., Kahru, M., Chao, Y., Rosenfeld, L. K., Bahr, F. L., et al. (2016). Initial skill assessment of the California Harmful Algae Risk Mapping (C-HARM) system. *Harmful. Algae.* 59, 1–18. doi: 10.1016/j.hal.2016.08.006

Anderson, C. R., Siegel, D. A., Brzezinski, M. A., and Guillocheau, N. (2008). Controls on temporal patterns in phytoplankton community structure in the Santa Barbara Channel, California. *J. Geophys. Res.* 113, 2007JC004321. doi: 10.1029/2007JC004321

Barron, J. A., Bukry, D., and Field, D. (2010). Santa Barbara Basin diatom and silicoflagellate response to global climate anomalies during the past 2200 years. *Quat. Int.* 215, 34–44. doi: 10.1016/j.quaint.2008.08.007

Bates, S. S., Bird, C. J., Freitas, A. S. W. D., Foxall, R., Gilgan, M., Hanic, L. A., et al. (1989). Pennate diatom Nitzschia pungens as the primary source of domoic acid, a toxin in shellfish from Eastern Prince Edward Island, Canada. *Can. J. Fish. Aquat.Sci.* 46, 1203–1215. doi: 10.1139/f89-156

Bates, S. S., Hubbard, K. A., Lundholm, N., Montresor, M., and Leaw, C. P. (2018). Pseudo-nitzschia, Nitzschia, and domoic acid: New research since 2011. *Harmful. Algae.* 79, 3–43. doi: 10.1016/j.hal.2018.06.001

Beatriz, R., and Eileen, B. (2023). *UNESCO harmful algae news NO.73.* (Paris: UNESCO). doi: 10.5281/ZENODO.8406488

Bejarano, A. C., VanDola, F. M., Gulland, F. M., Rowles, T. K., and Schwacke, L. H. (2008). Production and toxicity of the marine biotoxin domoic acid and its effects on wildlife: A review. *Hum. Ecol. Risk Assess.: An. Int. J.* 14, 544–567. doi: 10.1080/10807030802074220

Brunson, J. K., Thukral, M., Ryan, J. P., Anderson, C. R., Kolody, B. C., James, C. C., et al. (2024). Molecular forecasting of domoic acid during a pervasive toxic diatom bloom. *Proc. Natl. Acad. Sci. U.S.A.* 121. doi: 10.1073/pnas.2319177121

Capet, X., McWilliams, J. C., Molemaker, M. J., and Shchepetkin, A. F. (2008). Mesoscale to submesoscale transition in the California Current System. Part I: Flow structure, eddy flux, and observational tests. *J. Phys. Oceanogr.* 38, 29–43. doi: 10.1175/2007jpo3671.1

Chelton, D. B., Schlax, M. G., Freilich, M. H., and Milliff, R. F. (2004). Satellite measurements reveal persistent small-scale features in ocean winds. *Science* 303, 978–983. doi: 10.1126/science.1091901

Damien, P., Bianchi, D., Kessouri, F., and McWilliams, J. C. (2024). Extremes and short-term fluctuations in coastal ocean acidification and hypoxia. *JGR. Oceans.* 129, e2024JC021197. doi: 10.1029/2024JC021197

De La Riva, G. T., Johnson, C. K., Gulland, F. M. D., Langlois, G. W., Heyning, J. E., Rowles, T. K., et al. (2009). Association of an unusual marine mammal mortality event with Pseudo-nitzschia spp. blooms along the Southern California coastline. *J. Wildl. Dis.* 45, 109–121. doi: 10.7589/0090-3558-45.1.109

Deutsch, C., Frenzel, H., McWilliams, J. C., Renault, L., Kessouri, F., Howard, E., et al. (2021). Biogeochemical variability in the california current system. *Prog. Oceanogr.* 196, 102565. doi: 10.1016/j.pocean.2021.102565

Dong, C., Idica, E. Y., and McWilliams, J. C. (2009). Circulation and multiple-scale variability in the Southern California Bight. *Prog. Oceanogr.* 82, 168–190. doi: 10.1016/j.pocean.2009.07.005

Dong, C., and McWilliams, J. C. (2007). A numerical study of island wakes in the Southern California Bight. *Cont. Shelf. Res.* 27, 1233–1248. doi: 10.1016/j.csr.2007.01.016

Frieder, C. A., Kessouri, F., Ho, M., Sutula, M., Bianchi, D., McWilliams, J. C., et al. (2024). Effects of urban eutrophication on pelagic habitat capacity in the Southern California Bight. *Front. Mar. Sci.* 11. doi: 10.3389/fmars.2024.1392671

García-Reyes, M., and Largier, J. L. (2012). Seasonality of coastal upwelling off central and northern California: New insights, including temporal and spatial variability. *J. Geophys. Res.* 117. 47–59. doi: 10.1029/2011jc007629

García-Reyes, M., and Sydeman, W. J. (2017). California Multivariate Ocean Climate Indicator (MOCI) and marine ecosystem dynamics. *Ecol. Indic.* 72, 521–529. doi: 10.1016/j.ecolind.2016.08.045

Gibble, C. M., Kudela, R. M., Knowles, S., Bodenstein, B., and Lefebvre, K. A. (2021). Domoic acid and saxitoxin in seabirds in the United States between 2007 and 2018. *Harmful. Algae.* 103, 101981. doi: 10.1016/j.hal.2021.101981

Glibert, P. M., and Burford, M. A. (2017). Globally changing nutrient loads and harmful algal blooms: recent advances, new paradigms, and continuing challenges. *Oceanography* 30(1), 58–69.

Gómez-Ocampo, E., Gaxiola-Castro, G., Durazo, R., and Beier, E. (2018). Effects of the 2013–2016 warm anomalies on the California Current phytoplankton. *Deep. Sea. Res. Part. II: Top. Stud. Oceanogr.* 151, 64–76. doi: 10.1016/j.dsr2.2017.01.005

Heisler, J., Glibert, P. M., Burkholder, J. M., Anderson, D. M., Cochlan, W., Dennison, W. C., et al. (2008). Eutrophication and harmful algal blooms: A scientific consensus. *Harmful. Algae.* 8, 3–13. doi: 10.1016/j.hal.2008.08.006

Hoel, P., Moreno, A. R., and Bianchi, D. (2024). Mechanisms controlling lower trophic ecosystem response to ocean outfall discharges: role of nitrogen form and freshwater volume. *Reg. Stud. Mar. Sci.* 78, 103739.

Ho, M., Kessouri, F., Frieder, C. A., Sutula, M., Bianchi, D., and McWilliams, J. C. (2023). Effect of ocean outfall discharge volume and dissolved inorganic nitrogen load on urban eutrophication outcomes in the Southern California Bight. *Sci. Rep.* 13. doi: 10.1038/s41598-023-48588-2

Howard, M. D. A., Cochlan, W. P., Ladizinsky, N., and Kudela, R. M. (2007). Nitrogenous preference of toxigenic Pseudo-nitzschia australis (Bacillariophyceae) from field and laboratory experiments. *Harmful. Algae.* 6, 206–217. doi: 10.1016/j.hal.2006.06.003

Howard, M. D., Sutula, M., Caron, D. A., Chao, Y., Farrara, J. D., Frenzel, H., et al (2014). Anthropogenic nutrient sources rival natural sources on small scales in the coastal waters of the Southern California Bight. *Limnol. Oceanogr.* 59(1), 285–297.

Howard, M. D. A., Kudela, R. M., and McLaughlin, K. (2017). New insights into impacts of anthropogenic nutrients on urban ecosystem processes on the Southern California coastal shelf: Introduction and synthesis. *Estuar. Coast. Shelf. Sci.* 186, 163–170. doi: 10.1016/j.ecss.2016.06.028

Kahru, M., Jacox, M. G., and Ohman, M. D. (2018). CCE1: Decrease in the frequency of oceanic fronts and surface chlorophyll concentration in the California Current System during the 2014–2016 northeast Pacific warm anomalies. *Deep. Sea. Res. Part. I: Oceanogr. Res. Papers.* 140, 4–13. doi: 10.1016/j.dsr.2018.04.007

Kessouri, F., Bianchi, D., Renault, L., McWilliams, J. C., Frenzel, H., and Deutsch, C. A. (2020). Submesoscale currents modulate the seasonal cycle of nutrients and productivity in the California Current System. *Global Biogeochem. Cycl.* 34. doi: 10.1029/2020gb006578

Kessouri, F., McLaughlin, K., Sutula, M., Bianchi, D., Ho, M., McWilliams, J. C., et al. (2021a). Configuration and validation of an oceanic physical and biogeochemical model to investigate coastal eutrophication in the Southern California Bight. *J. Adv. Model. Earth Syst.* 13. doi: 10.1029/2020ms002296

Kessouri, F., McWilliams, J. C., Bianchi, D., Sutula, M., Renault, L., Deutsch, C., et al. (2021b). Coastal eutrophication drives acidification, oxygen loss, and ecosystem change in a major oceanic upwelling system. *Proc. Natl. Acad. Sci. U.S.A.* 118. doi: 10.1073/pnas.2018856118

Kessouri, F., Renault, L., McWilliams, J. C., Damien, P., and Bianchi, D. (2022). Enhancement of oceanic eddy activity by fine-scale orographic winds drives high productivity, low oxygen, and low pH conditions in the Santa Barbara Channel. *JGR. Oceans.* 127. doi: 10.1029/2022jc018947

Kessouri, F., Sutula, M. A., Bianchi, D., Ho, M., Damien, P., McWilliams, J. C., et al. (2024). Cross-shore transport and eddies promote large scale response to urban eutrophication. *Sci. Rep.* 14. doi: 10.1038/s41598-024-57626-6

Kvitek, R., Goldberg, J., Smith, G., Doucette, G., and Silver, M. (2008). Domoic acid contamination within eight representative species from the benthic food web of Monterey Bay, California, USA. *Mar. Ecol. Prog. Ser.* 367, 35–47. doi: 10.3354/meps07569

Lassiter, A. M., Wilkerson, F. P., Dugdale, R. C., and Hogue, V. E. (2006). Phytoplankton assemblages in the CoOP-WEST coastal upwelling area. *Deep Sea Res. II* 53(25-26), 3063–3077.

Lavaniegos, B. E., Jiménez-Pérez, L. C., and Gaxiola-Castro, G. (2002). Plankton response to El Niño 1997–1998 and La Niña 1999 in the southern region of the California Current. *Prog. Oceanogr.* 54, 33–58. doi: 10.1016/s0079-6611(02)00042-3

Lefebvre, K. A., Bargu, S., Kieckhefer, T., and Silver, M. W. (2002). From sanddabs to blue whales: the pervasiveness of domoic acid. *Toxicon* 40, 971–977. doi: 10.1016/s0041-0101(02)00093-4

Lefebvre, K. A., Kendrick, P. S., Ladiges, W., Hiolski, E. M., Ferriss, B. E., Smith, D. R., et al. (2017). Chronic low-level exposure to the common seafood toxin domoic acid causes cognitive deficits in mice. *Harmful. Algae.* 64, 20–29. doi: 10.1016/j.hal.2017.03.003

Lefebvre, L., Nicolakakis, N., and Boire, D. (2002). Tools and brains in birds. *Behav.* 139, 939–973. doi: 10.1163/156853902320387918

Lelong, A., Hégaret, H., Soudant, P., and Bates, S. S. (2012). Pseudo-nitzschia (Bacillariophyceae) species, domoic acid and amnesic shellfish poisoning: revisiting previous paradigms. *Phycologia* 51(2), 168–216.

Lévy, M., Couespel, D., Haëck, C., Keerthi, M. G., Mangolte, I., and Prend, C. J. (2024). The impact of fine-scale currents on biogeochemical cycles in a changing ocean. *Annu. Rev. Mar. Sci.* 16, 191–215. doi: 10.1146/annurev-marine-020723-020531

Lévy, M., Franks, P. J. S., and Smith, K. S. (2018). The role of submesoscale currents in structuring marine ecosystems. *Nat. Commun.* 9, 4069–4094. doi: 10.1038/s41467-018-07059-3

Lewitus, A. J., Horner, R. A., Caron, D. A., Garcia-Mendoza, E., Hickey, B. M., Hunter, M., et al. (2012). Harmful algal blooms along the North American west coast region: History, trends, causes, and impacts. *Harmful. Algae.* 19, 133–159. doi: 10.1016/j.hal.2012.06.009

Mantyla, A. W., Bograd, S. J., and Venrick, E. L. (2008). Patterns and controls of chlorophyll-a and primary productivity cycles in the Southern California Bight. *J. Mar. Syst.* 73, 48–60. doi: 10.1016/j.jmarsys.2007.08.001

Mason, E., Molemaker, J., Shchepetkin, A. F., Colas, F., McWilliams, J. C., and Sangrà, P. (2010). Procedures for offline grid nesting in regional ocean models. *Ocean. Modell.* 35, 1–15. doi: 10.1016/j.ocemod.2010.05.007

McCabe, R. M., Hickey, B. M., Kudela, R. M., Lefebvre, K. A., Adams, N. G., Bill, B. D., et al. (2016). An unprecedented coastwide toxic algal bloom linked to anomalous ocean conditions. *Geophys. Res. Lett.* 43. doi: 10.1002/2016gl070023

McClatchie, S., Goericke, R., Koslow, J. A., Schwing, F. B., Bograd, S. J., Charter, R., et al (2008). The state of the California Current, 2007–2008: La Niña conditions and their effects on the ecosystem. *CalCOFI Rep.* 49, 39–76.

McGregor, G. (2024). "Modes of climate variability," in *Heatwaves, biometeorology* (Springer International Publishing, Cham), 169–206. doi: 10.1007/978-3-031-69906-1_5

McKibben, S. M., Peterson, W., Wood, A. M., Trainer, V. L., Hunter, M., and White, A. E. (2017). Climatic regulation of the neurotoxin domoic acid. *Proc. Natl. Acad. Sci. U.S.A.* 114, 239–244. doi: 10.1073/pnas.1606798114

Moore, J. K., Doney, S. C., and Lindsay, K. (2004). Upper ocean ecosystem dynamics and iron cycling in a global three-dimensional model. *Global Biogeochem. Cycl.* 18, 2004GB002220. doi: 10.1029/2004GB002220

Moreno, A. R., Anderson, C., Kudela, R. M., Sutula, M., Edwards, C., and Bianchi, D. (2022). Development, calibration, and evaluation of a model of Pseudo-nitzschia and domoic acid production for regional ocean modeling studies. *Harmful. Algae.* 118, 102296. doi: 10.1016/j.hal.2022.102296

Nezlin, N. P., McLaughlin, K., Booth, J. A. T., Cash, C. L., Diehl, D. W., Davis, K. A., et al. (2018). Spatial and temporal patterns of chlorophyll concentration in the Southern California Bight. *JGR. Oceans.* 123, 231–245. doi: 10.1002/2017jc013324

National Water Research Institute (2024). *Independent expert review of the ROMS-BEC coastal ocean modeling system for Southern California coastal water-quality management.* (Fountain Valley, CA: National Water Research Institute).

NOAA National Geophysical Data Center (2003). *U.S. Coastal relief model vol.6 - southern california.* doi: 10.7289/V500001J

Radan, R. L., and Cochlan, W. P. (2018). Differential toxin response of Pseudo-nitzschia multiseries as a function of nitrogen speciation in batch and continuous cultures, and during a natural assemblage experiment. *Harmful. Algae.* 73, 12–29. doi: 10.1016/j.hal.2018.01.002

Rassweiler, A., Costello, C., and Siegel, D. A. (2012). Marine protected areas and the value of spatially optimized fishery management. *Proc. Natl. Acad. Sci. U.S.A.* 109, 11884–11889. doi: 10.1073/pnas.1116193109

Renault, L., Molemaker, M. J., McWilliams, J. C., Shchepetkin, A. F., Lemarié, F., Chelton, D., et al (2016). Modulation of wind work by oceanic current interaction with the atmosphere. *J. Phys. Oceanogr.* 46(6), 1685–1704.

Renault, L., McWilliams, J. C., Kessouri, F., Jousse, A., Frenzel, H., Chen, R., et al (2021). Evaluation of high-resolution atmospheric and oceanic simulations of the California Current System. *Prog. Oceanogr.* 195, 102564.

Sandoval-Belmar, M., Damien, P., Sutula, M., Kessouri, F., McWilliams, J., Ho, M., et al. (2026). Biogeochemical effects of Golden Gate Strait exchange and other land-based inputs to the San Francisco and Monterey Bay coasts. *JGR. Oceans.* 131, e2025JC023221. doi: 10.1029/2025JC023221

Sandoval-Belmar, M., Kessouri, F., Smith, J., Moreno, A. R., Anderson, C., Kudela, R. M., et al. (2026). Urban eutrophication enhances domoic acid production by Pseudo-nitzschia in the Southern California Bight. *Harmful. Algae.* 151, 103023. doi: 10.1016/j.hal.2025.103023

Sandoval-Belmar, M., Smith, J., Moreno, A. R., Anderson, C., Kudela, R. M., Sutula, M., et al. (2023). A cross-regional examination of patterns and environmental drivers of Pseudo-nitzschia harmful algal blooms along the California coast. *Harmful. Algae.* 126, 102435. doi: 10.1016/j.hal.2023.102435

Seegers, B. N., Birch, J. M., Marin, R., Scholin, C. A., Caron, D. A., Seubert, E. L., et al. (2015). Subsurface seeding of surface harmful algal blooms observed through the integration of autonomous gliders, moored environmental sample processors, and satellite remote sensing in southern California. *Limnol. Oceanogr.* 60, 754–764. doi: 10.1002/lno.10082

Sekula-Wood, E., Schnetzer, A., Benitez-Nelson, C. R., Anderson, C., Berelson, W. M., Brzezinski, M. A., et al. (2009). Rapid downward transport of the neurotoxin domoic acid in coastal waters. *Nat. Geosci.* 2, 272–275. doi: 10.1038/ngeo472

Sekula-Wood, E., Benitez-Nelson, C., Morton, S., Anderson, C., Burrell, C., and Thunell, R. (2011). Pseudo-nitzschia and domoic acid fluxes in Santa Barbara Basin (CA) from 1993 to 2008. *Harmful Algae* 10(6), 567–575.

Seubert, E. L., Gellene, A. G., Howard, M. D. A., Connell, P., Ragan, M., Jones, B. H., et al. (2013). Seasonal and annual dynamics of harmful algae and algal toxins revealed through weekly monitoring at two coastal ocean sites off southern California, USA. *Environ. Sci. pollut. Res.* 20, 6878–6895. doi: 10.1007/s11356-012-1420-0

Shchepetkin, A. F., and McWilliams, J. C. (2005). The regional oceanic modeling system (ROMS): a split-explicit, free-surface, topography-following-coordinate oceanic model. *Ocean. Modell.* 9, 347–404. doi: 10.1016/j.ocemod.2004.08.002

Skamarock, W. C., Klemp, J. B., Dudhia, J., Gill, D. O., Barker, D. M., Duda, M. G., et al. (2008). *A description of the advanced research WRF version 3* Vol. 475 (Boulder: Mesoscale and Microscale Meteorology Division. National Center for Atmospheric Research), 1. doi: 10.5065/D68S4MVH

Skelton, Z. R., McCormick, L. R., Kwan, G. T., Lonthair, J., Neira, C., Clements, S. M., et al. (2024). Organismal responses to deteriorating water quality during the historic 2020 red tide off Southern California. *Elem. Sci. Anth.* 12. doi: 10.1525/elementa.2023.00067

Smith, J., Cram, J. A., Berndt, M. P., Hoard, V., Shultz, D., and Deming, A. C. (2023). Quantifying the linkages between California sea lion (Zalophus californianus) strandings and particulate domoic acid concentrations at piers across Southern California. *Front. Mar. Sci.* 10. doi: 10.3389/fmars.2023.1278293

Smith, J., Gellene, A. G., Hubbard, K. A., Bowers, H. A., Kudela, R. M., Hayashi, K., et al. (2018). Pseudo-nitzschia species composition varies concurrently with domoic acid concentrations during two different bloom events in the Southern California Bight. *J. Plankton. Res.* 40, 29–45. doi: 10.1093/plankt/fbx069

Smith, J., Shultz, D., Howard, M. D. A., Robertson, G., Phonsiri, V., Renick, V., et al. (2021). Persistent domoic acid in marine sediments and benthic infauna along the coast of Southern California. *Harmful. Algae.* 108, 102103. doi: 10.1016/j.hal.2021.102103

Smith, J., Sutula, M., Lie, A. A. Y., and Weisberg, S. B. (2026). Harmful Algal Bloom Control in California Coastal Waters: January 12-13, 2026 Workshop Proceedings. *Technical Report 1463*. (Costa Mesa, CA: Southern California Coastal Water Research Project) .

Sutula, M., Ho, M., Sengupta, A., Kessouri, F., McLaughlin, K., McCune, K., et al. (2021). A baseline of terrestrial freshwater and nitrogen fluxes to the Southern California Bight, USA. *Mar. pollut. Bull.* 170, 112669. doi: 10.1016/j.marpolbul.2021.112669

Taylor, A. G., and Landry, M. R. (2018). Phytoplankton biomass and size structure across trophic gradients in the southern California Current and adjacent ocean ecosystems. *Mar. Ecol. Prog. Ser.* 592, 1–17.

Thessen, A. E., Bowers, H. A., and Stoecker, D. K. (2009). Intra- and interspecies differences in growth and toxicity of Pseudo-nitzschia while using different nitrogen sources. *Harmful. Algae.* 8, 792–810. doi: 10.1016/j.hal.2009.01.003

Thomas, A. C., Mendelssohn, R., and Weatherbee, R. (2013). Background trends in California Current surface chlorophyll concentrations: A state-space view: State-space trends in chlorophyll. *J. Geophys. Res. Oceans.* 118, 5296–5311. doi: 10.1002/jgrc.20365

Thompson, A. R., Swalethorp, R., Alksne, M., Santora, J. A., Hazen, E. L., Leising, A., et al. (2024). State of the California Current Ecosystem report in 2022: a tale of two La Niñas. *Front. Mar. Sci.* 11. doi: 10.3389/fmars.2024.1294011

Trainer, V. L., Kudela, R. M., Hunter, M. V., Adams, N. G., and McCabe, R. M. (2020). Climate extreme seeds a new domoic acid hotspot on the US west coast. *Front. Clim.* 2, 571836. doi: 10.3389/fclim.2020.571836.

Umhau, B. P., Benitez-Nelson, C. R., Anderson, C. R., McCabe, K., and Burrell, C. (2018). A time series of water column distributions and sinking particle flux of Pseudo-nitzschia and domoic acid in the Santa Barbara Basin, California. *Toxins* 10, 480. doi: 10.3390/toxins10110480

Wanninkhof, R. (1992). Relationship between wind speed and gas exchange over the ocean. *J. Geophys. Res.* 97, 7373–7388. doi: 10.1029/92jc00188

Zheng, B., Lucas, A. J., Franks, P. J. S., Schlosser, T. L., Anderson, C. R., Send, U., et al. (2023). Dinoflagellate vertical migration fuels an intense red tide. *Proc. Natl. Acad. Sci. U.S.A.* 120, e2304590120. doi: 10.1073/pnas.2304590120